

**Politecnico
di Torino**

Master's Degree in Environmental Engineering

Master's Degree Thesis

**The 'Mississippi River Delta
Transition Initiative':
Understanding the link between
plant salt stress and water table
dynamics in coastal wetlands**

Supervisor

Prof. Pierluigi Claps, Politecnico of Turin (Italy)

Candidate

Riccardo Della Corte

Co-supervisors

Prof. Annalisa Molini, Tulane University (USA)

Dr. Giulia Evangelista, Politecnico of Turin (Italy)

MARCH 2025

Abstract

Coastal wetlands have rapidly declined over the past 200 years due to human development, changes in land use, subsidence, sediment loss, rising sea levels, and shifts in hydro-climatic conditions. Approximately two-thirds of the world's coastal wetlands have vanished, with Louisiana accounting for about 40% of the U.S. coastal wetlands and 80% of the nation's total losses. From an ecohydrologic perspective, coastal wetlands are classified as Groundwater-Dependent Environments (GDEs). In these ecosystems, groundwater plays a critical role in sustaining life, and they have been extensively modeled using stochastic models of water table dynamics. However, the impacts of plant stress—particularly from salinization—on plant transpiration and the overall water budget of coastal wetlands remain largely unexamined. This thesis reviews and critically analyzes various modeling frameworks, comparing them with actual hydrological conditions. Specifically, the analysis focuses on coastal wetlands as a prototype for the ecosystems supporting the Mississippi River Delta (MRD) in Louisiana. This region provides a wide range of ecosystem services and serves as a vital economic and socio-political hub. Our findings emphasize the necessity for new modeling approaches that integrate the effects of salinization on ecosystem-scale transpiration, as well as temporal fluctuations in factors like salinity and sea level. Transitioning from a 'steady state' perspective to a 'time-dependent' approach promises a more accurate representation of these phenomena, which is essential for effectively supporting restoration and conservation efforts in these vulnerable areas.

Acknowledgements

I would like to express my heartfelt gratitude to my family for their unwavering support, and to my friends for their constant presence and encouragement throughout this long journey. I also extend my sincere appreciation to Dr. Emmanuel Ozioko for his invaluable support during my thesis project.

Table of Contents

Abstract	iii
Acknowledgements	v
Table of Contents	vii
List of Figures	ix
List of Tables	x
1 Introduction	1
2 Evolution Of Stochastic Models for Water Table Fluctuations in GDEs	8
3 Modeling the Water Table in SWT and Waterlogging Conditions Excluding Salinity Effects	16
3.1 Numerical Resolution Approach	17
3.2 Analytical Resolution Approach	20
3.2.1 Wieringermeer Effect and the Discrepancy with Experimental Data	21
4 Modeling the Water Table in SWT and Waterlogging Conditions with a Constant Salt Concentration	25
4.1 Salt Stress and Plant Adaptation Strategies	25
4.2 Analytical Resolution Approach Considering a Constant Salinity	27
5 Analysis and Interpretation of Real In Situ Data	33
5.1 Analysis of NOAA Data on Mean Sea Level Trends at Grand Isle	34
5.2 Analysis of Hydrological Conditions in the Birdfoot Area	36
5.3 Comparative Overview of Hydrological Conditions in the Terrebonne Basin	42
6 Conclusions	47
7 Code availability	50
Bibliography	51
A Dominant Vegetation in the Birdfoot	56
B Tools and methodologies for data collection	59

C	Process for changing data due to subsidence	64
D	Overview of Hydrological Conditions for MRD Stations	67

List of Figures

1.1	Satellite view of the modern MRD and the aerial view of the area . . .	5
1.2	Land changes along Louisiana’s coastline	6
2.1	Comparison by Pumo et al. (2010) between model-derived and empirical water table depths.	11
2.2	Comparison by Perri et al. (Under Review) of water table PDFs from models with and without salinity, and empirical data.	14
3.1	Comparison of PDFs derived from the numerical approach for the case study ‘Example’.	19
3.2	Comparison of PDFs derived from the numerical approach for the case study ‘NP46’.	19
3.3	Comparison of PDFs derived from the numerical approach for the case study ‘NP62’.	20
3.4	Comparison of PDFs derived from numerical and analytical approaches for the case study ‘Example’.	21
3.5	Comparison of PDFs derived from numerical and analytical approaches for the case study ‘NP46’.	22
3.6	Evolution of the Specific yield β as a function of the y value	23
4.1	Growth rate response to salinity stress for salt tolerant and sensitive plants.	26
4.2	Variation of transpiration as a function of salt concentration for three different plant species with different tolerance to saline conditions. . .	28
4.3	PDF variation of the water table with salinity for ”Phragmites australis” in the Everglades.	30
4.4	PDF variation of the water table with salinity for ‘Spartina patens’ in the Everglades.	31
4.5	[PDF variation of the water table with salinity for ‘Spartina alterniflora’ in the Everglades.	31
5.1	Monthly mean sea level measurements at Grand Isle (LA) and relative linear trend.	35
5.2	Spatial visualization of the various CRMS sites within the modern MRD.	37
5.3	Hydrological parameters and their temporal evolution for CRMS stations in the MRD.	39
5.4	Analysis of water table and salinity levels at monitoring station CRMS 0163.	40
5.5	Analysis of water table and salinity levels at monitoring station CRMS 2608.	41
5.6	Hydrological parameters and their temporal evolution for CRMS stations in the Terrebonne Basin.	43
5.7	Analysis of water table and salinity levels at monitoring station CRMS 0292.	44

5.8	Analysis of water table and salinity levels at monitoring station CRMS 0354.	45
A.1	Predominant vegetation for the different CRMS sites in the modern MRD	57
A.2	RGR and stem elongation in relation to salinity for Birdfoot's dominant species.	58
B.1	Photograph of a CRMS station designed for the measurement of open water table levels and various parameters.	60
B.2	Image of a frozen soil column employed in the assessment of land accretion processes.	62
B.3	RSET data collection scheme.	62
B.4	Image of a herbaceous marsh vegetation station and leveling rod.	63
C.1	Scheme of three possible scenarios regarding the subsidence of the RSET and the water level post.	65
C.2	Diagram indicating the correction of water level data to be implemented before and after the reference survey	66
D.1	Analysis of water table and salinity levels at monitoring station CRMS 0154.	67
D.2	Analysis of water table and salinity levels at monitoring station CRMS 0156.	68
D.3	Analysis of water table and salinity levels at monitoring station CRMS 0157.	68
D.4	Analysis of water table and salinity levels at monitoring station CRMS 0159.	69
D.5	Analysis of water table and salinity levels at monitoring station CRMS 0161.	69
D.6	Analysis of water table and salinity levels at monitoring station CRMS 0162.	70
D.7	Analysis of water table and salinity levels at monitoring station CRMS 2634.	70

List of Tables

- 3.1 Parameter values used in the case studies in Tamea et al. (2010) . . . 17
- 4.1 Salt tolerance parameters for the three plant species analyzed in this study 30

Chapter 1

Introduction

Coastal wetlands are often defined by citing the definition created by the Ramsar Convention¹, i.e., as areas of marsh, bog, or fens with static or flowing water, fresh, brackish, or salt, including sites of seawater no deeper than 6 meters. They are usually found near the interface between land and sea, such as tidal marshes and mangrove swamps [Scott et al. (2014)], and are formed by tidal forces, freshwater inputs, and especially the transport of sediment and biota [Zhao et al. (2016)]. They constitute 38% of the total area of wetlands in the contiguous United States, with a higher concentration in the southeast of the country², particularly in the Gulf of Mexico (GOM) Engle (2011). In these regions, the soils have a high water content, resulting in the exclusion of the air present in the porous medium, leading to anoxic conditions. This intensely affects vegetation that has adopted morphological and physiological changes to survive [Van Huyssteen (2023)]. Wetlands are crucial for the environment and human well-being, providing several ecosystem services. However, assigning monetary values to each of them is complicated, facilitating decisions about protecting, restoring, and mitigating these areas [Engle (2011)].

First of all, they are of great importance in coastal protection from storm surges, allowing, in technical terms, the reduction of wave heights (cm) during the wave crossing phase (km^{-1}). This is made possible by emergent vegetation and shallow water depths, which absorb wave energy and thus reduce and slow their motion [Engle (2011)]. The latter also acts as a barrier to prevent direct wind impact on the water table, thus limiting the creation of swells [Costanza et al. (2008)]. According to

¹<https://www.ramsar.org/>

²<https://www.epa.gov/wetlands/about-coastal-wetlands#whatAre>

the original report by the US Army Corps of Engineers (USACOE), thanks to these ecosystems, there was an average reduction in storm surges of 7.0 cm km^{-1} during seven hurricanes that struck Louisiana between 1907 and 1957³.

Another benefit of these habitats is their ability to remove nitrogen from surface waters, significantly reducing the tendency for eutrophication processes in coastal areas. Moreover, this process improves these environments' growth, productivity, and functionality, consequently increasing the amount of other ecosystem services they perform [Engle (2011)].

They are also characterized by their capacity to sequester and store so-called 'Blue Carbon,' i.e., the organic carbon captured and held by the oceans and coastal ecosystems, mainly vegetated. It is of particular interest concerning combating climate change and improving shoreline protection and fisheries [Macreadie et al. (2019)]. The high productivity of these environments implies a rapid growth of vegetation, which captures significant amounts of carbon in the form of carbon dioxide (CO_2). They can also be defined as carbon sinks due to the soil's anoxic characteristics, which slow down the decomposition of organic material and reduce its subsequent release back into the atmosphere. It has been estimated that the average rate of organic carbon sequestration in coastal wetlands can reach up to $210 \text{ g m}^{-2} \text{ year}^{-1}$ on a ten to one hundred year scale [Hao et al. (2024)].

Growing urbanization along coastal areas also increasingly makes these territories hotspots of immense animal and plant species biodiversity, many of which are defined as threatened or endangered⁴.

Despite their critical importance, the extent of coastal wetlands worldwide declined by more than 50% during the 20th century. Focusing on the United States, the loss rate of these areas between 1780 and 1980 resulted in some states losing more than 80% of their tidal wetlands, with the most significant reduction occurring in the country's southeastern regions during the 1970s [Li et al. (2018)]. It is clear that this issue is relevant and complicated to manage, as the causes are numerous and interconnected. Climate change-related consequences, such as an increase in average temperature, changes in rainfall distribution and intensity, and sea level change, are some factors contributing to these habitats' disappearance [Day et al. (2008)]. According to modeling of possible future scenarios (IPCC, 2007)⁵, the latter will be, on

³<https://www.mvn.usace.army.mil/>

⁴<https://www.fws.gov/program/endangered-species>

⁵<https://www.ipcc.ch/report/ar4/wg1/>

average, 28-43 cm higher at the end of the 21st century compared with its value at the beginning of the century. It is important to note that the interactions among flooding, plant growth, and elevation changes stabilize submerged wetlands, enabling these ecosystems to adapt to rising sea levels [Kirwan and Megonigal (2013)]. The vertical growth of the marsh surface can equal or even exceed that of the sea, thus ensuring the survival of the marsh vegetation [Reed (1995)]. This feedback can be analyzed in two domains: above and below the ground surface. In the former, the deposition of numerous mineral sediments occurs during tidal flooding with a contribution proportional to the submergence time. Still, it is also related to the presence of plant shoots, which act as obstacles to water flow and add organic material to the soil. In the subsoil, on the other hand, elevation is caused by roots, characterized by a balance between growth and decomposition [Kirwan and Megonigal (2013)]. Nevertheless, this represents a general perspective rather than a discourse applicable in all contexts. It is essential to point out that coastal marshes are being converted to open water in areas characterized by low altitudes and high relative sea level rise trends, such as the northern coasts of the GOM. In these zones, tidal inundation has the opposite effect to that described above, with a reduction in organic matter contributions and major erosive processes [Kirwan and Megonigal (2013)]. In addition to causes that could be described as resulting from 'natural' processes, human activities are largely responsible for the disappearance of these ecosystems. Groundwater withdrawal and artificial soil drainage led to high levels of subsidence, especially in the southern-east part of the United States [Kirwan and Megonigal (2013)]. At these two points, the intense hydrocarbon extraction process in the GOM should be added, which is closely linked to the rates of land surface degradation recorded in areas such as Grand Isle (LA) and Galveston (TX) [Kolker et al. (2011)]. Furthermore, the increase in the number of dams and reservoirs to better control the course of rivers is reducing the inflow of runoff to the coast, with an estimated 20 % reduction globally. Finally, direct human intervention is the primary factor contributing to the destruction of coastal wetlands, both historically and in modern times. Indeed, despite decades of research and awareness campaigns emphasizing the importance of addressing this issue, the problem persists [Kirwan and Megonigal (2013)]. In particular, these ecosystems are subject to drainage or filling for agriculture and human settlements, resulting in the loss of soil organic carbon (SOC) and the release of CO_2 into the atmosphere as well as greenhouse gases such as CH_4 and nitrous oxide (N_2O), thus increasing the prob-

lem of climate change and accelerating the issues related to phenomena previously defined as 'natural,' hence leading to a vicious circle. [Huang et al. (2010)].

The following thesis will focus in particular on the analysis of coastal wetlands in the Mississippi River Delta (MRD), which has received increasing attention from various experts in different fields, such as engineering or biology, due to the extreme importance of the river itself, the ecosystem present in the delta, the economic value it represents for the state of Louisiana and the entire nation, together with the significant vulnerability that characterized it [Coleman J (1998)].

The delta formation process, which began around 5000 BC, did not occur uniformly but underwent several changes over time [Coleman J (1998)], with various sub-deltas (or lobes) that followed and overlapped each other throughout the centuries, creating a large wetland area along the coast of Louisiana. The formation and disappearance of these sub-deltas are closely linked to the course of the Mississippi River, which changed its path several times, cutting a shorter route towards the Gulf of Mexico. The lack of sediment and freshwater input led to a significant increase in subsidence, erosion, and compaction rates in the lobe, resulting in its abandonment in favor of forming a new one [Coleman J (1998)]. In particular, several studies have stated that there are specific stages defined in the life cycle of the MRD [Roberts (1997)], and these include: initiation and creation of the delta, systematic reduction of flow efficiency and sediment dispersion, abandonment of the delta due to changes in the river course, and modification of the perimeter of the abandoned delta (influenced by sea level rise and subsidence phenomena). In the end, the entire delta area consists of at least six delta complexes that have succeeded each other over time: Maringouin/Sale Cypremort, Teche, St. Bernard, LaFourche, Atchafalaya-WaxLake, and Balize [Coleman J (1998)]. Their progression has impacted a region along the southern Louisiana coastline, covering around 22,000 km² (2.2 million ha), thus creating the seventh largest river delta in the world, made up of more than 11,000 km² (1.1 million ha) of coastal wetlands [Olson and Suski (2021)].

In addition, the modern configuration of the delta, where the river actually meets the GOM, forming one of the most dynamic and vulnerable areas in the world, covers approximately 2,107 km² (521,000 ac) and is known as the Balize or Plaquemines-Balize Delta (Figure 1.1). This region is distinguished by a unique shape that resembles the outline of a bird's foot, which has led to its nickname "Birdfoot"⁶.

⁶https://lacoast.gov/new/about/basin_data/mr/default.aspx



Figure 1.1: The left panel shows the satellite view of the modern MRD (NASA website), while the right panel depicts the aerial view of the area (Delta Discovery Tours website).

The latter can be further divided into four sub-deltas: West Bay, Cubit’s Gap, Baptiste Collette, and Garden Island Bay. Each of these develops through the natural process of levee breaches and follows a specific life cycle that includes periods of growth and decline [Coleman J (1998)]. Its structure comprises a complex and interconnected network of channels, and within it, the river branches out primarily in three distinct directions: Southwest Pass (west), Pass A Loutre (east), and South Pass (center)⁷. Information on the predominant vegetative species in this region relies on data collected by the Coastwide Reference Monitoring System⁸ (CRMS) , which detects significant changes in plant composition caused by the responses of these plants to transformations in their habitats. The prevalent species are *Phragmites australis* and *Sagittaria lancifolia* L. [Coleman J (1998)], whose characteristics are briefly described in Appendix A.

It is important to emphasize that the modern MRD represents a fundamental economic and sociopolitical resource. Commercial fishing activities are highly prevalent, and numerous petrochemical complexes make it the world’s most significant raw materials port. Furthermore, since it is mainly made up of coastal wetlands, this area is of significant environmental importance, as it provides many of the ecosystem services mentioned above [Day et al. (2024)]. Despite this, it is one of the most vul-

⁷<https://www.mvd.usace.army.mil/Media/Images/igphoto/2000759695/>

⁸<https://www.lacoast.gov/crms/>

nerable areas regarding land loss. Between 1932 and 2016, the Louisiana coastline experienced an estimated reduction of 4,833 km² (about 25% of its original area) [Couvillion et al. (2017)], with the most significant challenges in the delta, where the total area diminished over the last 60 years has been around 458 km² (113,300 acres)⁹.

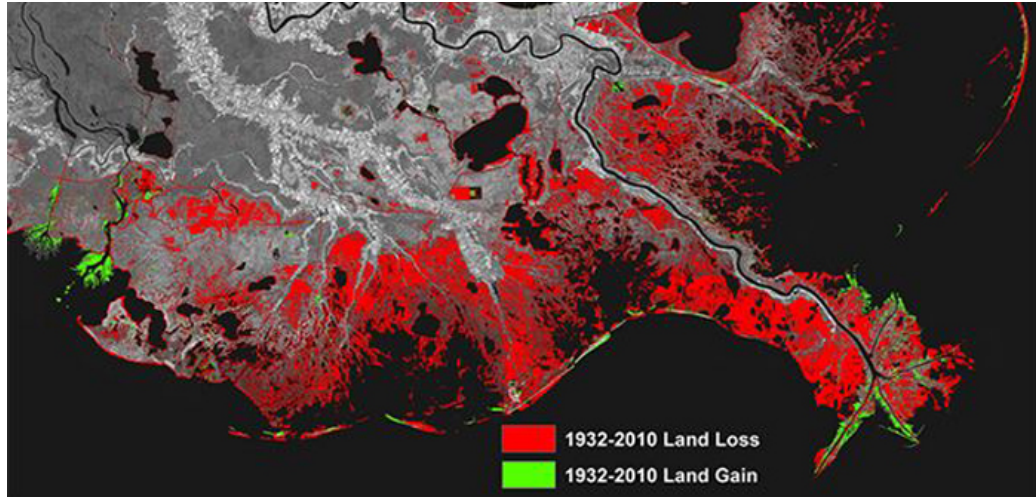


Figure 1.2: Map depicting land changes along a significant portion of Louisiana’s coastline, with the most severe land loss observed in the Balize Delta (NASA Sea-Level Rise Impact).

Human impacts on the MRD are numerous, many of which are associated with the presence of a strong oil and gas (O&G) industry, which is among the largest globally, with about 20% of crude oil and 33% of natural gas for the entire nation originating from this area [Davis and Guidry (1996)]. Over 30,000 km of artificial channels have been dredged in less than a century to facilitate and enable access to the various extraction wells. This has led to a series of catastrophic consequences for the existing ecosystem, including altering natural hydrology and salinity, which reduces the exchange of sediments and organic matter. Evidently, this also impacts the existing vegetation, reducing its productivity. Additionally, by removing fluids from the subsoil, fuel extraction increases the subsidence rate and activates geological faults, thereby accelerating land loss [Day et al. (2020)]. Finally, the construction of levees and structures to mitigate flooding has altered the distribution of sediments within the Mississippi, resulting in a substantial decrease in their delivery to the coastal wetland, diminishing their ability to cope with subsidence rates and rising sea levels [Day et al. (2020)].

It is also important to highlight the aspect related to sediment management along

⁹https://lacoast.gov/new/about/basin_data/mr/default.aspx

the Gulf Coast of the United States, an innovative practice has recently emerged that is based on harnessing the sediment that is dredged into channels for navigability issues (amounting to approximately 65 million cubic meters each year) and using it as a resource for restoring coastal ecosystems, thus attempting to combat subsidence in the region. This practice consists of dredging sediments from the bottom of navigation channels and using them to nourish the region's wetlands and restore riverbanks through direct deposition. A clear example of this method is the West Bay diversion restoration project in the Mississippi Delta, in which the innovative combination of an uncontrolled sediment diversion and the strategic and direct placement of the dredged materials allows for the entrainment of the latter from the diversion flow and subsequent sedimentation. This system has already created 8 km^2 (800 ha) of new land, with an increase of 6.46 km^2 (646 ha) between 2005 and 2020 alone [Suedel et al. (2021)]. The benefits of this practice can be summarized into three main classes: economic, social, and environmental. On the economic side, there are lower costs related to the process and placement of dredging and a decrease in eventual expenditures for the maintenance of navigation channels. In the social sphere, the project fully supports the development of recreational activities in the area. Finally, the most critical aspect concerns the environmental domain, allowing the transformation of territories, previously in open water state, into wetlands with a higher elevation than in ordinary tidal conditions. This alteration fosters the growth of more resilient plant communities, enhancing the overall resilience of the region [Suedel et al. (2021)]. Despite the efforts and positive progress, it is still difficult to cope with the rate of soil loss recorded in the delta, which is caused by the whole series of impacts listed above.

Considering the information provided thus far, studying and protecting coastal wetland ecosystems is paramount, especially in the Balize Delta. Many processes occur within these habitats, but this study aims to analyze, understand, and predict the dynamics of the variation of the water table and how interconnected external factors, such as salinity and vegetation presence, influence it.

Chapter 2

Evolution Of Stochastic Models for Water Table Fluctuations in GDEs

The category of environment identified in the area under review falls within the so-called 'Groundwater-dependent environments' (GDEs), i.e. ecosystems in which groundwater plays a fundamental role in regulating vegetation dynamics and soil water balance [Laio et al. (2009)]. The interactions among soil, climate, and vegetation significantly influence, and are in turn shaped by, the depth of groundwater and soil moisture levels. Fluctuations in aquifer depth and moisture gradients within the porous medium are pivotal to ecohydrological processes such as infiltration, runoff, groundwater flow, land surface-atmosphere exchanges, vegetation dynamics, nutrient cycling, and pollutant transport. Analyzing these interactions is both an advanced and complex area of research, complicated by the erratic and unpredictable nature of precipitation. This variability introduces stochastic dynamics that tightly couple soil moisture and groundwater fluctuations, highlighting the inherent challenges of studying these interconnected systems [Pumo et al. (2010)]. Given the strong dependence on groundwater resources and their vulnerability to external influences, several models have been developed over time that aim to describe the stochastic dynamics of the water table through probabilistic approaches, expressed through probability density functions (PDF). These models explore the interactions between the movement of water in the ground, both in saturated and unsaturated zones, considering the random elements that condition these mechanics.

What follows is a summary of the main research work that has been carried out

in this area, with focus on steady-state conditions and their applications. Before proceeding, however, it is necessary to clarify a basic concept for a proper understanding of the subject. Specifically, the variable \tilde{y} refers to the water level, i.e. the saturated soil surface at zero pressure. On the other hand, $y(t)$ denotes the interface between the saturated and unsaturated zones of the soil, which is always a constant distance above the water table, and is equal to ψ_s , where ψ_s is the saturated matric potential of the soil, with a negative value. The relationship between these two quantities is expressed as:

$$y(t) = \tilde{y}(t) - \psi_s \quad (2.1)$$

For practical reasons, in the context of modeling groundwater dynamics, we prefer to use $y(t)$, as it is more appropriate to the theoretical frameworks used [Laio et al. (2009)].

From the first traditional models, the focus was initially on arid or semi-arid ecosystems, far away from environments such as wetlands. This approach often neglected the interaction between the water table and vegetation, assuming that the water table's depth was inaccessible to it, which clearly influenced the types of species present. By not considering the reciprocal effect between the water table and plants, this assumption limited the understanding of ecological dynamics [Pumo et al. (2010)].

In the work of Ridolfi et al. (2008), a significant initial step is taken in the analysis of stochastic soil water balance in GDEs. The present research proposes an analytical probabilistic model that aims to describe soil moisture dynamics on a daily basis, taking into account both bare soil conditions and the presence of a shallow water table (SWT). The proposed model considers variables such as random rainfall distribution, water table fluctuations, capillary rise and soil evaporation. However, it should be noted that this framework has not yet been adapted for the case of vegetative soil.

To address this lacuna, Laio et al. (2009) propose a significant advancement by introducing a new model that allows the dynamics of the water table depth to be represented probabilistically, taking into account interactions with plant roots in both saturated and unsaturated zones. The evolution of the y can thus be described using univariate stepwise-continuous first-order stochastic differential equations, thereby incorporating randomness into the system, particularly through the introduction of a multiplicative random Poisson noise term, which reflects the distribution of precip-

itation. The solution to these equations is derived under steady-state conditions, thereby facilitating the evaluation of the probability density function of the water table depth $p_Y(y)$ (Formula 2.2).

$$p_Y(y) = \frac{C}{f(y)} \exp \left[- \int_0^y \frac{f(u) + \alpha \lambda(u) g(u)}{\alpha g(u) f(u)} du \right] \quad (2.2)$$

with C a normalization constant due to $\int_{-\infty}^0 p_Y(y) dy = 1$, $\alpha \lambda(u)$ is the noise average and $f(u)$, $g(u)$ are two stepwise functions.

However, this model relies on a purely hydraulic approach and fails to consider the effects of salinity on the plants, which can be significant in coastal wetland environments. Although it accounts for deep water table (DWT) scenarios, such instances are infrequent in Louisiana coastal wetlands where the water table typically remains near or even above the surface. The model operates under steady-state conditions, which are reached when the system is in equilibrium and therefore does not take into account the temporal variation of variables such as sea level y_0 , and it involves several simplifying assumptions. For instance, soil properties, such as effective porosity (n), grain size distribution, and water retention curves, are assumed to be spatially uniform and temporally constant. The area of interest is assumed to be relatively flat, which is reasonable given the typically flat nature of wetlands. Local heterogeneity in soil and vegetation, as well as topographic gradients or regional groundwater dynamics, are not taken into account. Additionally, the effect of evaporation is neglected, as it is small compared to transpiration when dense vegetation is present [Laio et al. (2009)].

This study was validated in Pumo et al. (2010), using real data to identify processes potentially overlooked by the conceptual framework, providing valuable insights for future enhancements. The evaluation involved applying the model at three selected sites within Everglades National Park, Florida, based on long-term daily records of groundwater depth, precipitation, and evapotranspiration. Site 1, located near Florida Bay, is influenced by oceanic conditions, while Sites 2 and 3, situated in the Frog Pond Area and near levee L31W respectively, are affected by nearby canals. The chosen sites exhibit water level fluctuations confined to the shallow soil layer, ensuring that standing water is either absent or present only briefly, which aligns with the framework's limitations. Two approaches for parameter aggregation are considered: one uses annual averages for evapotranspiration, rainfall, and external water levels,

while the other distinguishes between the dry season (December to May) and wet season (June to November), applying separate input parameters for each (Figure 2.1).

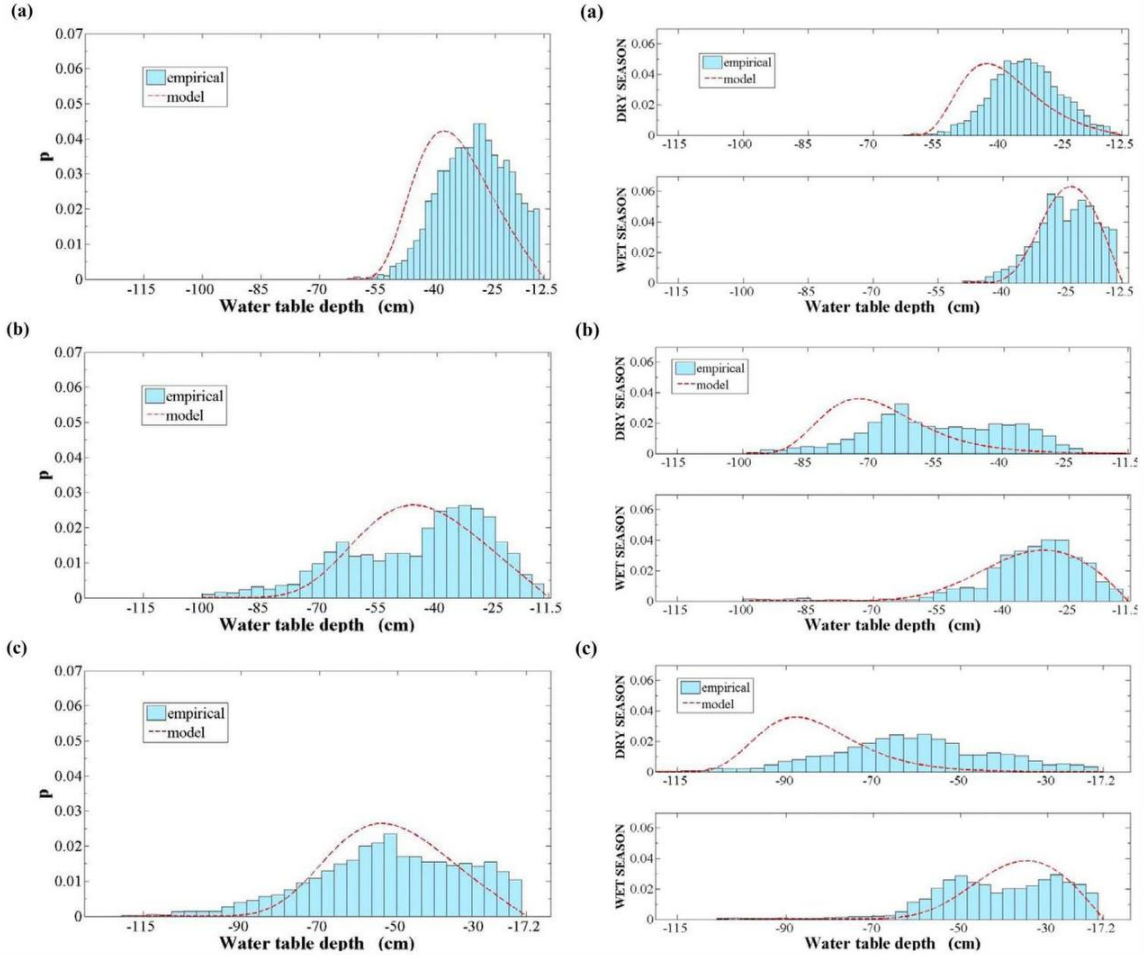


Figure 2.1: PDF of the water table depths obtained from the model compared with empirical depths. Annual analysis in the left column and seasonal analysis in the right column for Site 1 (a), Site 2 (b) and Site 3 (c). Reproduced from Pumo et al. (2010).

In the annual analysis, the model assumes constant external water levels y_0 and utilizes average annual conditions, which limits its ability to account for seasonal variations and lateral flow dynamics. In this case, it is possible to conclude that the model approximates the empirical data reasonably well, although it slightly underestimates both the depth and variability of the water table, generating distributions that are more symmetric compared to the often asymmetric and bimodal observed patterns. In the seasonal analysis, the model continues to assume stable external water levels, despite the significant daily and seasonal fluctuations in the adjacent

canals. At Site 1, it effectively reproduces the PDF; however, for Sites 2 and 3, this accuracy decreases. Specifically, during the dry season, the model predicts a deeper water table, whereas in the wet season, it forecasts shallower levels. This discrepancy is more pronounced during the dry season, primarily due to prolonged dry spells, the lasting influence of initial conditions, and reduced rainfall frequency, all of which delay the stabilization of the system and consequently hinder the model's ability to provide accurate prediction (Pumo et al. (2010)).

Subsequently, for completeness, it is important to introduce the simple process-based stochastic framework developed by Tamea et al. (2009) for soil moisture dynamics. This study, which takes into account climate, vegetation, and soil properties, allows the probability distribution function of soil moisture $s(z^*)$ to be derived, thereby complementing the stochastic model of groundwater depth previously discussed. Citing this study is crucial as it provides valuable insights into the interactions between soil moisture and key hydrological processes, such as water redistribution, groundwater recharge, and capillary flow from the water table to unsaturated soil layers. Furthermore, in the presence of vegetation, the study highlights the significant role of root water uptake in regulating the local soil water balance, thereby influencing overall moisture levels (for a detailed analysis, refer to [Tamea et al. (2009)]). Nevertheless, within the context of the coastal wetland under investigation, where the soil profile is almost entirely saturated due to the presence of shallow groundwater, the dynamics of soil moisture in the unsaturated zone become less relevant. Given the persistent near saturation of these systems, the importance of the model is somewhat constrained. However, its inclusion remains significant in ensuring the comprehensiveness of the broader hydrological analysis.

Returning to the discussion of water table dynamics, the model proposed by Laio et al. (2009) does not account for waterlogging (WL) scenarios, which occur when the water table remains above the soil surface for extended periods (hydroperiods). This can lead to significant damage to vegetation by impairing root aeration and altering plant growth. Such a simplification proves problematic in coastal wetlands, especially in the Birdfoot area, where submersion is a common and recurring event. Therefore, WL represents a critical issue that should not be overlooked in this context.

To address this issue, the theoretical framework proposed by Tamea et al. (2010) considers the stochastic variations of the water table, including the possibility of it exceeding the ground surface. In particular, in the context of WL conditions,

the authors analytically solve the long-term probability density function of the water table (Formula 2.2) and show that it takes the form of a Pearson III-type distribution. These enhancements enable the resulting approach to generate a PDF of the water table that more closely reflects real-world field data, despite still being based on steady-state conditions. The proposed approach was then validated by comparing it to data from monitoring stations in Everglades National Park (Florida, USA). A more detailed examination of this framework will be presented in the following chapter.

To conclude, a critical aspect overlooked by the models discussed so far, yet essential for analyzing probabilistic changes in the water table of coastal regions, is the growing concern of saltwater intrusion, which has negative effects on vegetation. This phenomenon is further exacerbated by submersion due to rising sea levels and changes in local hydrological regimes, significantly impacting coastal wetlands, particularly in Louisiana, which are already vulnerable due to subsidence and human activities.

To address this issue, a salinity-dependent soil water balance model was developed by Perri et al. (Under Review), incorporating stochastic recharge events and accounting for SWT conditions. The study reveals that plants with higher salt tolerance can maintain a deeper water table compared to less tolerant species under identical salinity conditions; however, once salinity surpasses a critical threshold, even the most salt-tolerant species experience stress, which leads to a reduction in transpiration. This decline not only affects the transpiration rates of the vegetation but also impairs the plants' ability to regulate the water table, causing groundwater fluctuations to become increasingly reliant on changes in sea level. Consequently, a linear correlation emerges between sea level y_0 and groundwater levels, complicating the prediction and management of water availability.

This analysis further compared empirical data from four sites in the southeastern Everglades (collected from 1996 to 2020) with two models: the stochastic water budget model that does not account for salinity (as previously proposed) and the current salinity-constrained model. The results clearly showed that the model ignoring salinity failed to replicate the observed water table distributions, while the salinity-constrained model closely matched the empirical data. This was particularly evident in the dry season, where salt stress played a dominant role, leading to shallower water tables more frequently than predicted by the non-salinity model. During the wet season, the differences between the two models were less pronounced due to the dilution of salinity from freshwater inputs and the rise in sea level due to thermal expansion.

Nonetheless, the salinity-dependent model generally predicted deeper water tables in the wet season, as salinity levels approached optimal conditions for transpiration. Overall, this salinity-constrained g model proved to be far superior, offering a much more accurate representation of water table dynamics in these coastal ecosystems, particularly during periods of elevated salinity stress (Figure 2.2).

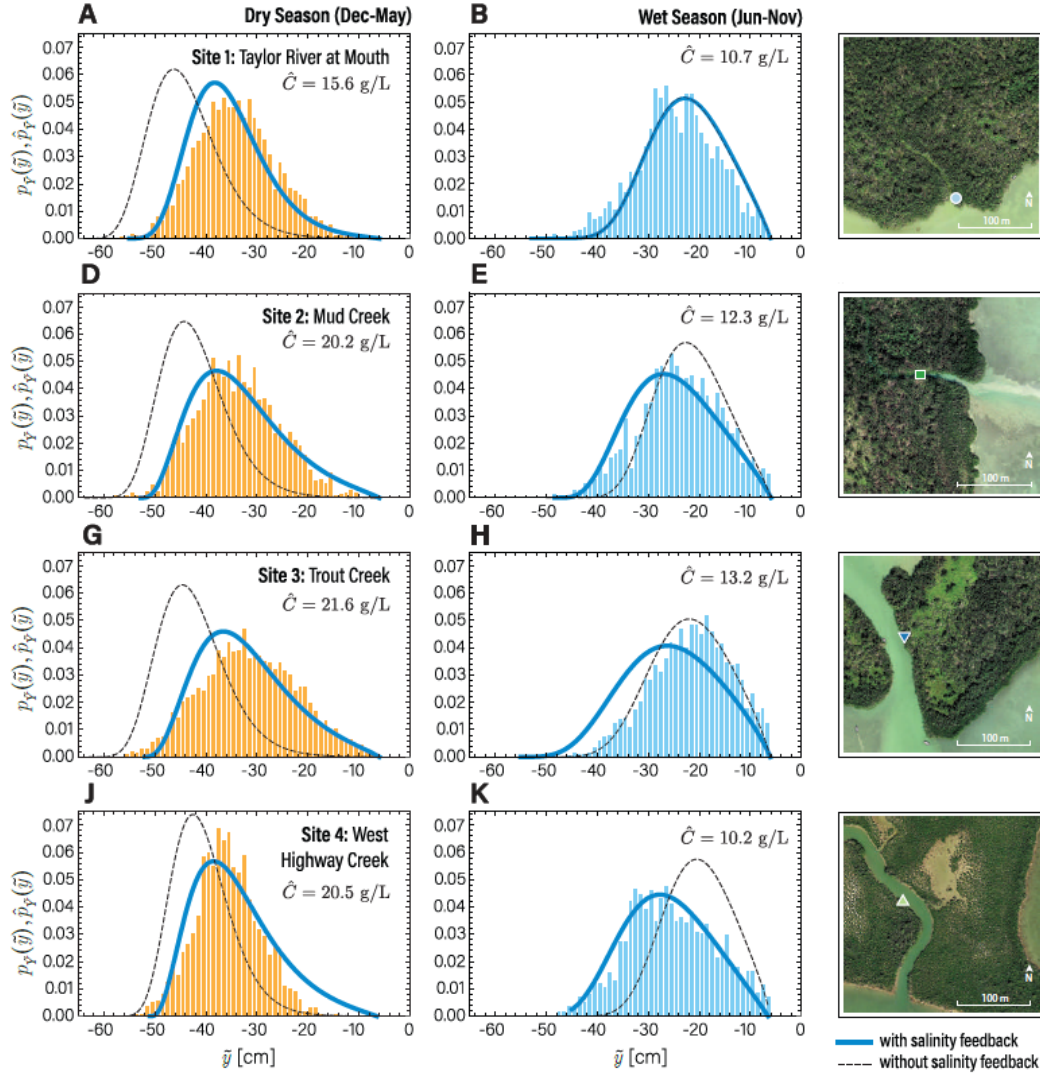


Figure 2.2: Comparison of the probability distribution from the two models with the empirical PDFs at the four examined sites. The solid blue line represents the model with salinity feedback, whereas the dashed line represents the model without. Additionally, the image provides an aerial view of the location for each site. Reproduced from Perri et al. (Under Review)

As previously discussed, studies conducted over time have progressively sought to incorporate additional factors to provide a more accurate representation of the empirical data. However, it should be emphasized that all of these investigations

assume steady-state conditions; that is to say, they operate under the assumption that the system reaches an equilibrium state. In this specific case, this implies that the water table remains at a relatively constant level, with fluctuations reduced to a minimum. To overcome this limitation and effectively model a transient system, such as that observed in real scenarios, it is necessary, on the basis of existing research, to develop a stochastic numerical model that takes into account variations in variables such as salinity and sea level y_0 .

Chapter 3

Modeling the Water Table in SWT and Waterlogging Conditions Excluding Salinity Effects

As anticipated in the previous part, over time there has been a growing production of studies aimed at analyzing the variation of the water table in wetlands, with the intention of predicting its evolutionary trends. This chapter is purely theoretical in nature and aims to reproduce and analyze approaches that have been widely used in the past to determine the pdf of the water table, under salinity-free assumptions, without considering vegetation characteristics. The first phase of the work followed a numerical approach, using the methodology proposed in [Tamea et al. (2010)]. The subsequent stage adopted an analytical procedure, yielding a solution analogous to that previously obtained through numerical methods.

All the solutions considered in the following come from the water balance equation Laio et al. (2009), whose terms will be examined in detail in the following section:

$$\beta(y) \frac{dy}{dt} = Re(y, t) - ET(y) + f_i(y) \quad (3.1)$$

The models were implemented using the software 'Wolfram Mathematica', and the corresponding codes are provided in Chapter 7.

3.1 Numerical Resolution Approach

The approach outlined in Tamea et al. (2010) was implemented for the three case studies considered ("Example", "NP46", "NP62"), with the corresponding data provided in Table 3.1. The method used involves substituting the expressions for the various terms, which vary depending on the specific condition (DWT/SWT/WL), into the probability density function of the water table proposed (Formula 3.2). Subsequently, a numerical solution of the PDF was obtained, combining the solutions for the "above-ground" and "underground" cases. These merged results were then normalized across the entire domain of interest to ensure that the area under the curve was equal to 1, thus guaranteeing the validity of the probability density function.

$$p_Y(y) = \frac{C \cdot \beta(y)}{ET(y) - fl(y)} \exp \left\{ - \int_0^y \left[\frac{\beta(u)}{\alpha} - \frac{\lambda_0 \beta(u)}{ET(u) - fl(u)} \right] du \right\} \quad (3.2)$$

Although the focus of this analysis is on the SWT and WL conditions, which are strongly dominant in the Birdfoot area, DWT conditions have also been included for this particular phase only. This allows a direct comparison with the actual on-site conditions, where deep water levels are possible. However, it should be noted that the considerations and formulations for the DWT case are not included in this discussion as they are not relevant to the following investigation. The depth that separates deep from shallow groundwater is commonly referred to in the literature as the critical depth, denoted as y_c . For further information, please refer to Laio et al. (2009).

Table 3.1: Parameter values used in the case studies in Tamea et al. (2010)

	λ_0 (d ⁻¹)	α (cm)	ET_{\max} (cm d ⁻¹)	b (cm)	y_0 (cm)	k_1 (d ⁻¹)	$k_{1,2}$ (d ⁻¹)	soil	n (-)	ψ_s (cm)	m (-)	k_s (cm d ⁻¹)
Example	0.30	1.2	0.4	20	-20	0.007	0.007	loam	0.463	-11	0.22	31
NP46	0.589	0.95	0.48	10	0	0.001	0.006	m-peat	0.5	-10	0.20	10
NP62	0.607	0.97	0.46	10	-20	0.001	0.003	m-peat	0.5	-10	0.20	10

The 'Specific yield', denoted by β , is defined as the ratio between the volume of water released or stored by an aquifer (V_w) per unit area and the corresponding change in the depth of the water table (Δy) Laio et al. (2009). The corresponding formulation under SWT and WL conditions is presented below. It is important to note that under conditions of complete soil flooding ($y > 0$), this term is obviously assumed to be equal to unity, implying that there is a direct proportionality between the groundwater level and the volume of water that is added or extracted.

$$\beta(y) = \begin{cases} n - n \left[1 + \left(s f c^{-\frac{1}{2m}} - 1 \right) \left(\frac{y}{y_c} \right) \right]^{-2m} & \text{if } y < 0, \\ 1 & \text{if } y \geq 0. \end{cases} \quad (3.3)$$

The term f_l is used to indicate lateral flows, which have been shown to exert a significant influence on the variation of the water table level. These occur in the presence of a nearby water body (the sea in this case) and their direction and intensity are contingent on the difference between the water table level y and the ocean level y_0 Laio et al. (2009).

$$f_l(y) = \begin{cases} k_l(y_0 - y - \psi_s) & \text{if } y < 0, \\ k_{l,2}(y_0 - y) & \text{if } y \geq 0. \end{cases} \quad (3.4)$$

It is clear that for an accurate representation of the phenomenon it is essential to distinguish between flow in the porous medium ($y < 0$) and flow above the soil surface ($y > 0$), as the dynamics are different.

ET denotes evapotranspiration, which encompasses the combined processes of evaporation from soil and plant surfaces and transpiration through the plant's stomata Kar et al. (2016). Under SWT and WL conditions, and in the absence of salt influence, water availability in the soil is assumed to be unlimited. As a result, evapotranspiration reaches its maximum value, ET_p , since it is not constrained by either water stress or salt stress, and is therefore assumed to be at its full capacity Tamea et al. (2010).

Finally, the terms α and λ represent two parameters associated with the stochastic forcing of precipitation. On a daily scale, precipitation follows a marked Poisson process, dependent on the mean annual precipitation frequency λ (1/day) and the mean annual rainfall height α (cm). Under SWT and WL conditions, both parameters are considered constants, since each rainfall input contributes to the recharging of the water table. However, under DWT conditions, other factors such as infiltration and water redistribution in the soil column must be taken into account Laio et al. (2009).

As can be seen in Figure 3.1, Figure 3.2 and Figure 3.3, there is a high correlation between the results obtained by the two solutions. In the case of the "Example", the curve of the solution that also includes the DWT shows a peak below ground level that is shifted towards less negative values of \tilde{y} , but with a greater amplitude compared to the case that only considers SWT and WL. The peak obtained by the

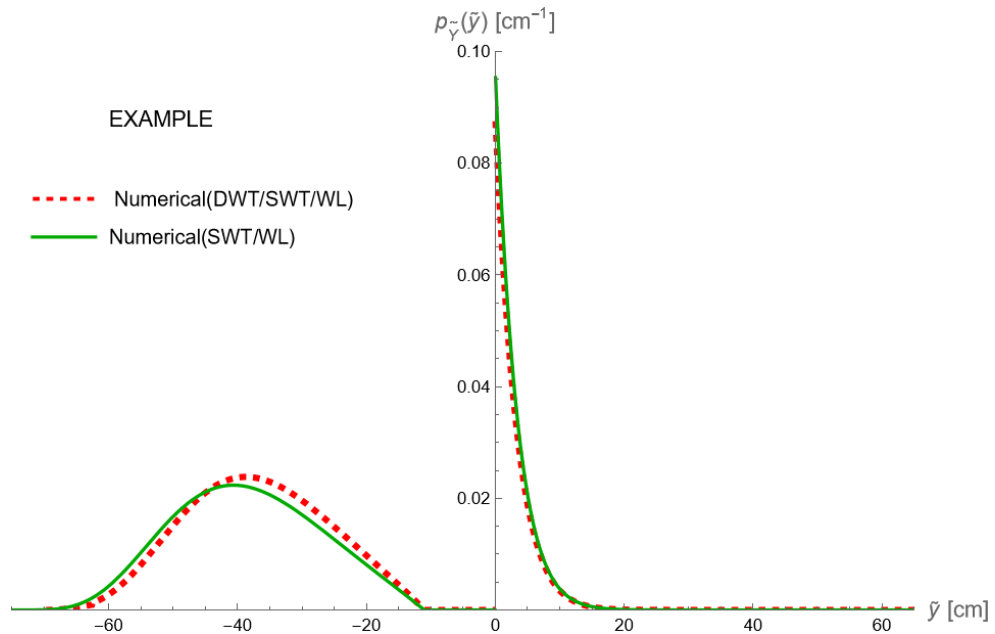


Figure 3.1: Comparison of the PDFs of the water table, derived from the numerical approach for the case study "Example" considering DWT, SWT, and WL conditions (red dotted line) and SWT and WL conditions only (green continuous line).

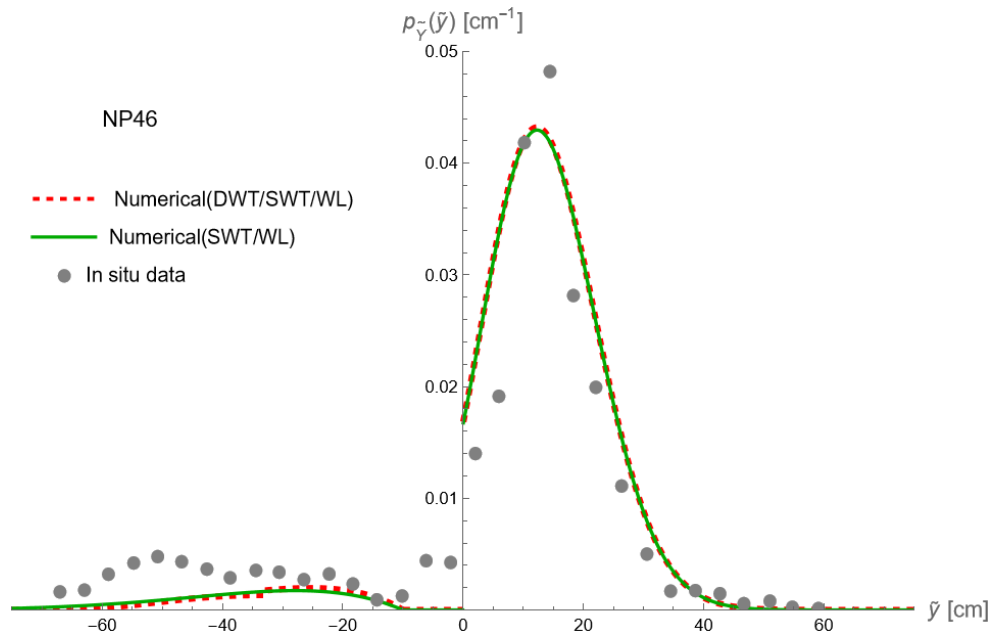


Figure 3.2: Comparison of the groundwater table PDF derived from the numerical approach for case study 'NP46' considering DWT, SWT and WL conditions (dashed red line) and SWT and WL conditions only (solid green line). The actual values collected in situ are indicated by grey dots.

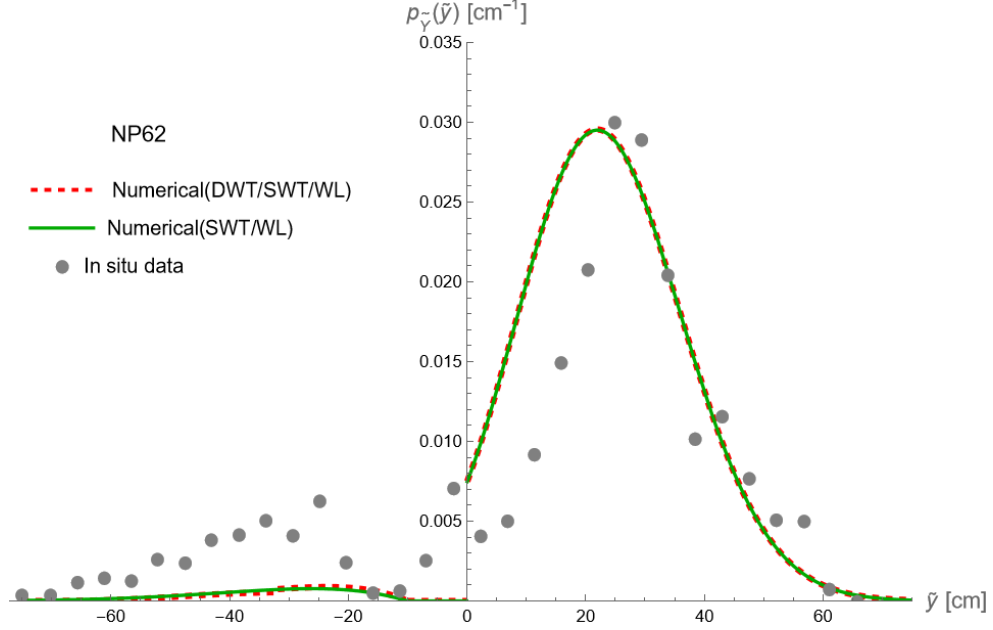


Figure 3.3: Comparison of the groundwater table PDF derived from the numerical approach for case study ‘NP62’ considering DWT, SWT and WL conditions (dashed red line) and SWT and WL conditions only (solid green line). The actual values collected in situ are indicated by grey dots.

solution including DWT has slightly lower $p_{\tilde{Y}}(\tilde{y})$ values, as can be observed from the situation above ground. This result is quite plausible and is related to the fact that neglecting conditions where the water table can reach significant depths leads to a greater tendency for the water table to rise above ground level. This phenomenon produces an increase in the PDF area for $\tilde{y} > 0$. It is noteworthy that these considerations hold true for the stations designated as ‘NP46’ and ‘NP62’; however, the two solutions are almost indistinguishable in their respective case studies, as the water level at these stations rarely falls below a depth of y_c .

3.2 Analytical Resolution Approach

Over time, various analytical formulations have been suggested regarding the PDF of the water table. Therefore, we began our analysis with the solution proposed in Perri et al. (Under Review), which focuses solely on the SWT condition and does not take into account salt concentration. In addition, the generic expression of the probability density function (Formula 3.2) was analytically solved for the specific case of flood conditions, leading to a significant simplification of the expression and the

integral within it. The two solutions were then combined and normalized over the entire domain of interest. As in the previous section, the data from Table 3.1 were used, with the final solutions illustrated by a blue line in Figure 3.4 for the Example and in Figure 3.5 for the NP46 scenario.

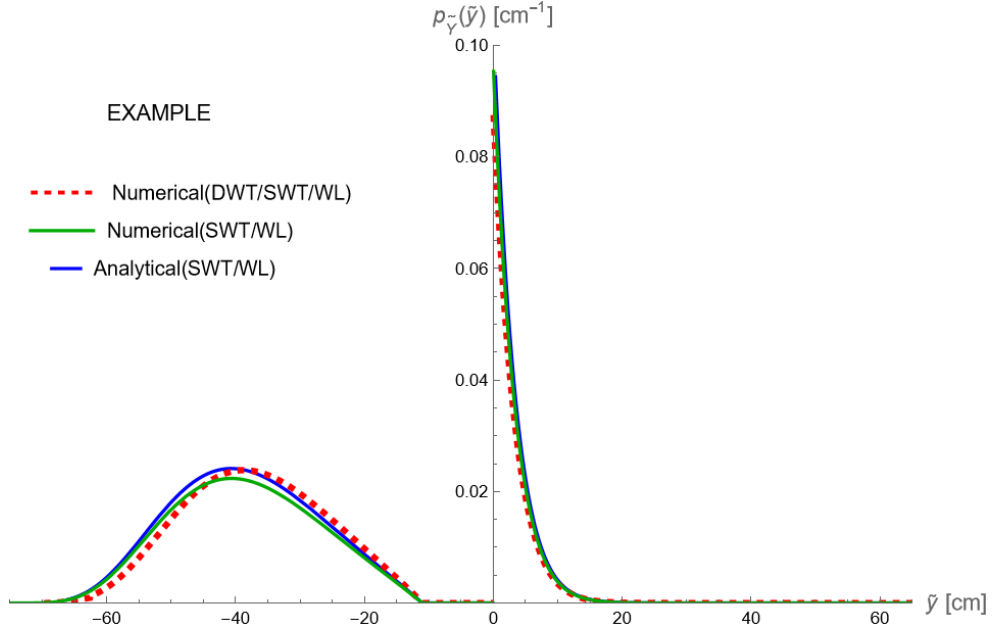


Figure 3.4: Comparison of the groundwater table PDF for case "Example", obtained by analytical approach under SWT and WL conditions (blue continuous line) and by numerical resolution (red dashed line and green continuous line).

However, case study NP62 was not included in the discussion because the analytical solution derived showed an incorrect trend, even though the process adopted is the same. This is most likely attributable to the instability of the solutions used, causing certain combinations of input values to create problems and compromise the reliability of the solution.

In both the cases analysed, the analytical approach demonstrate a strong correspondence with the previously derived numerical solutions. Although small discrepancies are observed, these are attributable to errors in the approximations used during the numerical process. where the software does not produce an exact solution of the integral, but employs a certain degree of approximation.

3.2.1 Wieringermeer Effect and the Discrepancy with Experimental Data

It is interesting to note that, in both theoretical approaches analysed, a jump in $p_{\tilde{y}}(\tilde{y})$ occurs in the proximity of the soil surface, obviously more or less marked

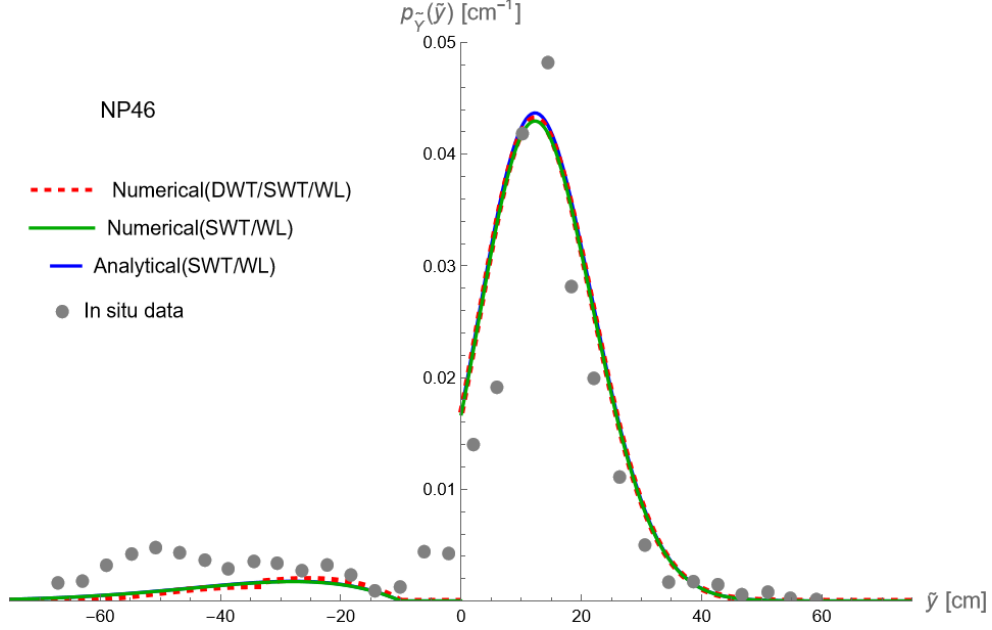


Figure 3.5: Comparison of the groundwater table PDF for case "NP46", obtained by analytical approach under SWT and WL conditions (blue continuous line) and by numerical resolution (red dashed line and green continuous line). The actual values recorded in situ are indicated by grey dots.

depending on the type of case study considered. This phenomenon is referred to as the ‘Wieringermeer effect’ [Heliotis and DeWitt (1987)], i.e. a process due to the fact that if a completely saturated soil column is considered, this simultaneously corresponds to having $\tilde{\gamma}=0$ and $\tilde{\gamma}=\psi_s$, implying that during the table ascent there is a pressure jump from ψ_s to 0 without a volume change.

Furthermore, above the ground surface, each addition or extraction of water results in a corresponding and equal shift in the depth of the water table, hence the parameter $\beta=1$. In contrast, in a porous medium, changes in the water table level are significantly influenced by capillary forces, especially near the surface. In this case, even small changes in water volume can cause large shifts in the position of the water table, resulting in potential instability. This explains the discontinuity in the final solutions, indicating that conditions of complete saturation without flooding are highly unlikely [Tamea et al. (2010)].

This discrepancy is less evident in the experimental data, which show a more gradual transition. This is probably due to the fact that the theoretical model used (for both approaches) assumes an ideal soil column, i.e. undisturbed by external factors and uniform, which differs from real in situ conditions. In fact, in real conditions, the

water present in macropores is released when the level inside the piezometer falls, filling the measurement well and partially attenuating the sudden change in the position of the free surface. An additional mechanism is associated with the gradual response of the piezometer itself to changes in the water table, leading to a progressive release of water into the surrounding soil, thus increasing local moisture levels [Tamea et al. (2010)].

In the Birdfoot area, these probability jumps at the soil-atmosphere interface are made even less obvious by the use of indirect and approximate instruments to measure groundwater levels (for more information see the appendix C).

Finally, still referring to the discontinuity in the theoretically derived PDF, this is closely related to the trend of the Specific yield, which decreases and approaches 0 as the water table rises towards the surface. This is correct and inherent in the definition of the term, as the capacity of the porous medium to store or release water is reduced. Whereas above ground, the volume change of water per unit area is obviously equal to the variation in water table height, and thus forced to be equal to 1 (Figure 3.6).

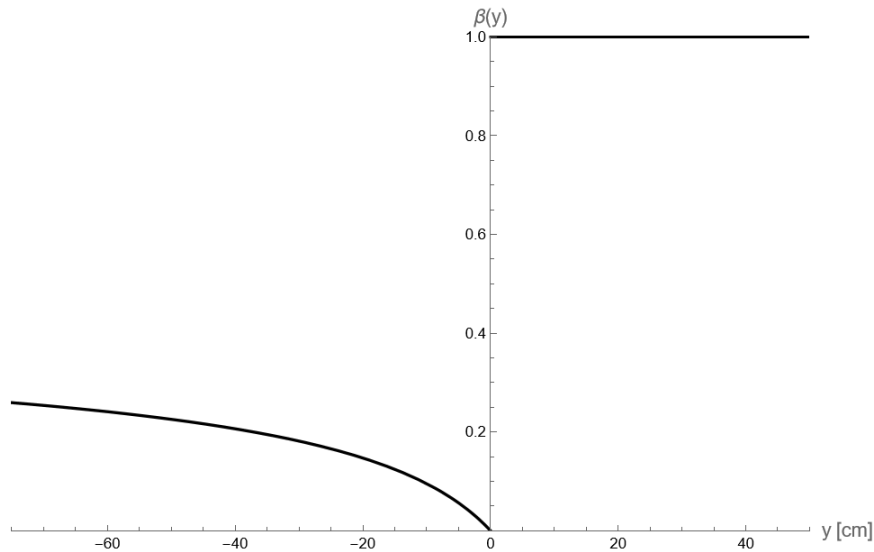


Figure 3.6: Evolution of the Specific yield β as a function of the y value

Although this is conceptually valid, in reality the transition between above and below ground is smoother and the trend is site-specific.

An attempt was therefore made to estimate the effect of the beta trend for some of the Birdfoot stations using an approach derived from the so-called 'White method', i.e. a technique normally used to estimate the level of evapotranspiration in flooded wetlands. In particular, it proposes different strategies, depending on the data avail-

able, to derive the so-called Ecosystem Specific Yield (ESY), which describes the evolution of the parameter as a function of the water table, assuming, however, that the area under consideration is not flat but morphological a basin. This assumption can be safely associated with the MRD area, as the instruments are positioned in open water, and therefore in a zone that is depressed in any case. In particular, the ESY_R approach was used, which aims to empirically estimate β values by correlating the ratio R_R of net rainfall (taking into account interception) and the corresponding rise in groundwater level, thus relying on the general definition of the term but using empirical data [Mclaughlin and Cohen (2014)]. However, the lack of sufficient rainfall records and the absence of a direct correlation between precipitation and water level changes for the MRD area led to erroneous and inconclusive results. In fact, rain data are collected at hourly intervals from an eddy covariance station (USGS LA3, located in Barataria Bay) and compared with water level measurements from the nearest CRMS station (CRMS 3166).

Chapter 4

Modeling the Water Table in SWT and Waterlogging Conditions with a Constant Salt Concentration

4.1 Salt Stress and Plant Adaptation Strategies

In the models presented above, the effect of salinity on vegetation is not considered, although this is very relevant, especially in coastal wetlands where the intrusion of saline water is a strong present phenomenon. Salinization can negatively impact a plant's ability to regulate the water table, leading to various detrimental effects. It can limit soil aeration and hinder nutrient uptake by vegetation, affecting its establishment and survival. Additionally, salt can increase the plants' exposure to submer-sion conditions, which can create hypoxic environments and lead to the accumulation of toxic substances [Perri et al. (Under Review)]. The extent of the phenomenon may vary depending on climatic conditions, light intensity, plant species, or soil type [Acosta-Motos et al. (2017)].

Thus, in the presence of excessive concentrations of Na^+ and Cl^- , there are two stresses to which the plant is subjected (Figure 4.1):

- **Osmotic stress:** It generally occurs in the first few minutes/hours (depending on the salt concentration C and the species present). As C increases, there is a reduction in the soil water potential, which implies that, despite the availability

of groundwater, water is less accessible to the roots due to the osmotic bonds it forms with dissolved salts Parida and Das (2005), mainly affecting evapotranspiration with a consequent reduction in the stomatal conductance of the leaves and compromising plant growth. In general, the characteristics of this phenomenon are very similar to those of water stress conditions Perri et al. (2018).

- **Ionic stress:** This phenomenon is salt-specific and occurs when the plant is subjected to prolonged salinity conditions over time (days/weeks), leading to cellular damage due to the presence of toxic salts in plant tissues Nobel (1983), causing damage that mainly affects the leaf apparatus of the specimen, such as senescence of old leaves and reduction of the photosynthetic leaf area Perri et al. (2018).

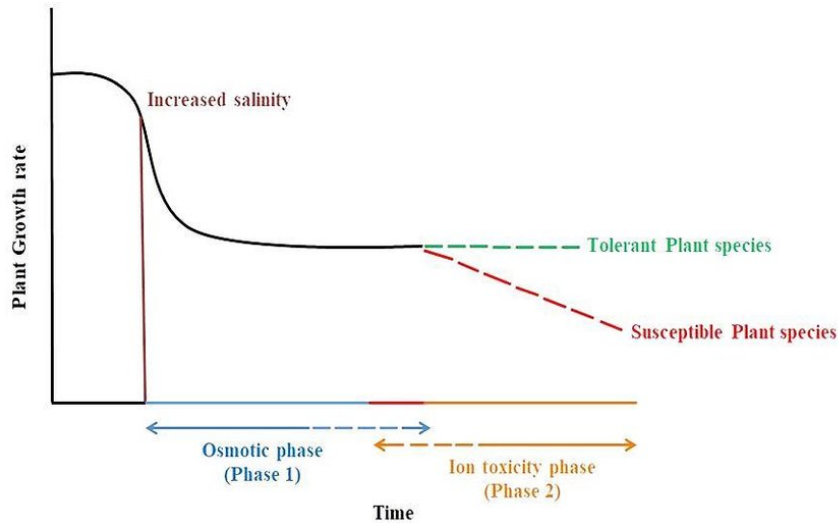


Figure 4.1: Growth rate response to salinity stress (osmotic and ionic phase) for salt tolerant and sensitive plants. Reproduced from [Polash et al. (2019)].

However, different plant species adopt a variety of survival mechanisms in response to the stresses just described, and depending on whether or not they can grow in saline environments, these are classified as Glycophytes or Euhalophytes. The former, which include the majority of cultivable plants, cannot grow in the presence of salt, and their development is inhibited or even completely stunted even at minimal NaCl concentrations (100-200 mM), leading to the specimen's death. In contrast, the latter can grow even in more pronounced saline conditions (300-500 mM of NaCl), thanks to various strategies presented below [Acosta-Motos et al. (2017)].

First, after an initial passive phase of dehydration lasting a few minutes with a

consequent increase in osmolyte concentration, the plant shows a certain tolerance to osmotic stress, actively regulating water flows through the so-called osmotic adjustment until it reaches a certain equilibrium in which it can continue to grow, although at a reduced rate, adapting to saline conditions [Perri et al. (2018)]. A second mechanism involves salt exclusion at the root level, with the roots filtering the absorbed water to reduce the amount of salt entering the plant. Finally, ionic compartmentalization consists of accumulating Na^+ and Cl^- at the cellular and intracellular levels, thus preventing the build-up of toxic ion concentrations within the cytoplasm [Perri et al. (2018)]. If, on the other hand, one focuses on longer time scales (several weeks or more), salt-tolerant species can develop various morphological adaptations, including small leaves, a high root area index (RAI) - which represents the root area per unit of soil surface - leaf succulence and high water use efficiency [Perri et al. (2018)].

Depending on the type of plant considered, there may be a different relationship between Tr (plant transpiration) and C , which is often used to define and compare the different tolerances of species. The optimum growth and transpiration rate is reached at a certain level of $CT_{r,max}$, which is higher the less salt-sensitive the species is [Perri et al. (Under Review)]. It should be noted that this value is usually medium/high for halophytes, so they may be exposed to stresses specific to freshwater, and beyond this threshold, transpiration and productivity begin to decrease. It should also be noted that this pattern becomes less pronounced with prolonged exposure and the consequent onset of morphological adaptations [Perri et al. (2018)].

4.2 Analytical Resolution Approach Considering a Constant Salinity

The inclusion of the salinity effect in the analytical model to determine the PDF of the groundwater level does not involve a significant variation in the underlying logical process presented in the previous chapter 3, and the underlying soil water balance remains similar (Formula 3.1). However, since salt implies a change in the expression of evapotranspiration, this is no longer always constant and maximum but instead depends on the value of C and the type of plant species considered. Moreover, since DWT conditions are assumed not to be present in this discussion, ET is independent of the variable y .

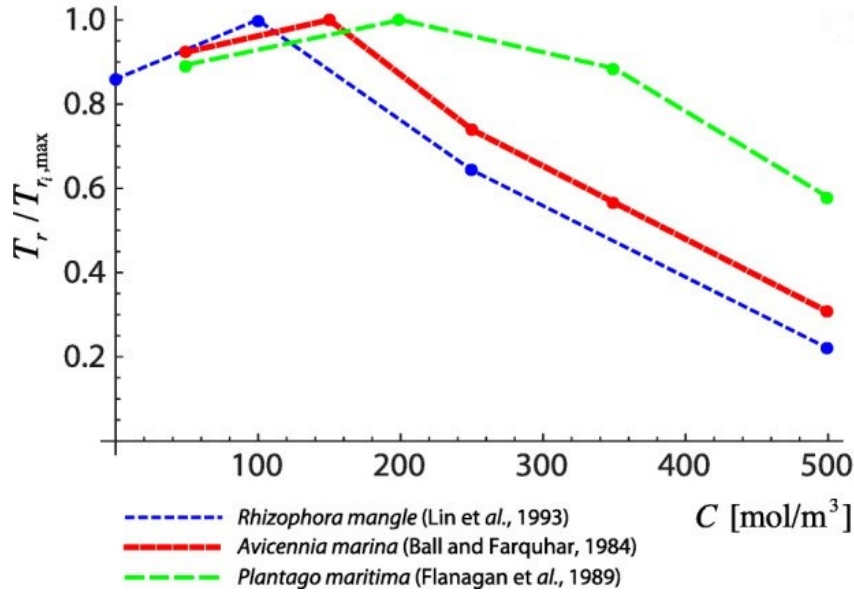


Figure 4.2: Variation of actual transpiration (T_r) from maximum transpiration ($T_{r,max}$) as a function of salt concentration (C , expressed in mol/m^3) for three different plant species with different tolerance to saline conditions. It is observed that maximum transpiration is reached for non-zero salt concentrations, reflecting the stress present in freshwater conditions. Also note that the higher the salt tolerance, the higher the salt concentration at which maximum transpiration is reached and the lower the curve slope beyond the peak. Reproduced from Perri et al. (2018)

The proposed model assumes that the dependence of ET on C can be described by a threshold model inspired by the Maas-Hoffman salinity reduction function. In this context, it is assumed that for salinity concentrations below the species-specific threshold $CT_{r,max}$, water uptake by the plant reaches the maximum possible value. Conversely, uptake is assumed to decrease linearly with increasing salinity concentration for salinity levels above this specific limit [Skaggs et al. (2014)]. Therefore, a simplified approach is adopted with respect to the generic scheme shown in Figure (4.2) above, omitting the stress due to fresh water.

The salinity reduction function $f(C)$ [Perri et al. (Under Review)] is expressed as:

$$f(C) = \begin{cases} 1 & C \leq C_{Tr_{max}} \\ 1 - \beta(C - C_{Tr_{max}}) & C > C_{Tr_{max}} \end{cases} \quad (4.1)$$

and the limit imposed by salinity on ET can be formulated as:

$$ET(C) = ET_p \begin{cases} 1 & C \leq C_{Tr_{max}} \\ 1 - \phi\beta(C - C_{Tr_{max}}) & C > C_{Tr_{max}} \end{cases} \quad (4.2)$$

ET_p represents the potential evapotranspiration that a given plant species can achieve under optimal conditions. At the same time, the term ϕ refers to an estimate of the ratio between actual transpiration (T_r) and potential evapotranspiration (ET_p) based on plant cover and in this case is assumed equal to 1. Furthermore, β is another key indicator, together with $C_{Tr_{max}}$, based on which the uptake reduction function in the threshold model is constructed. Specifically, it describes the rate at which transpiration decreases as salinity increases and is lower the greater the plant's salt tolerance. The parameters for a specific species can be estimated by referencing tables that outline the salt tolerance values of various plants [Perri et al. (Under Review)].

The analytical approach to obtain the probability distribution of the water table was then re-proposed, following a similar procedure for the case without salinity but including, in this case, the reduction of evapotranspiration as a function of C. For the PDF concerning the water table, the analytical expression presented in [Perri et al. (Under Review)] was adopted, while for the inundation state, the Formula 3.2 was again solved analytically. Once again, the two solutions were combined, and the final result was normalized.

Due to the absence of soil hydraulic and precipitation data in the Birdfoot area, a purely theoretical approach was chosen to analyse the effects of salinity on the water table. The model requires the same input parameters used in the framework described in Chapter 3. However, in this case, the values were taken from a hypothetical site within Everglades National Park, assumed to be sufficiently similar to those of the MRD area, thus allowing for a consistent analysis of the hydrological dynamics. However, the vegetation considered includes three species prevalent in the Louisiana coastal area: *Phragmites australis*, *Spartina alterniflora*, and *Spartina patens*. All three exhibit low salt tolerance, and their values defining the $f(C)$ function are provided in Table 4.1. In particular, the parameter β was obtained through a linear fit of the values available in the literature.

In the three cases analyzed (Figure 4.3, Figure 4.4, Figure 4.5), a significant aspect is that as the salt concentration increases (which in this case reaches purely theoretical values that do not reflect the actual in situ conditions), the area of the PDF shifts to

Table 4.1: Salt tolerance parameters for the three plant species analyzed in this study

Species	$CT_{r,max}$	β
Phragmites australis	3.55	0.0542
Spartina alterniflora	5.84	0.0175
Spartina patens	5.00	0.0391

the right, indicating a greater possibility of SWT conditions or complete soil flooding. This behavior is in line with the previously investigated theoretical framework and is related to reduced plant transpiration in saline environments.

Furthermore, at the equivalent C values, more tolerant species, such as "Spartina alterniflora", show a smaller PDF shift than less tolerant species, such as "Phragmites australis". Finally, for C values below $CT_{r,max}$, note how the curves coincide. The reason for this is linked to the inherent simplification of the model and the formulation adopted (Formula 4.2), which assumes a maximum and constant value of evapotranspiration under these conditions, although this is not the case in reality.

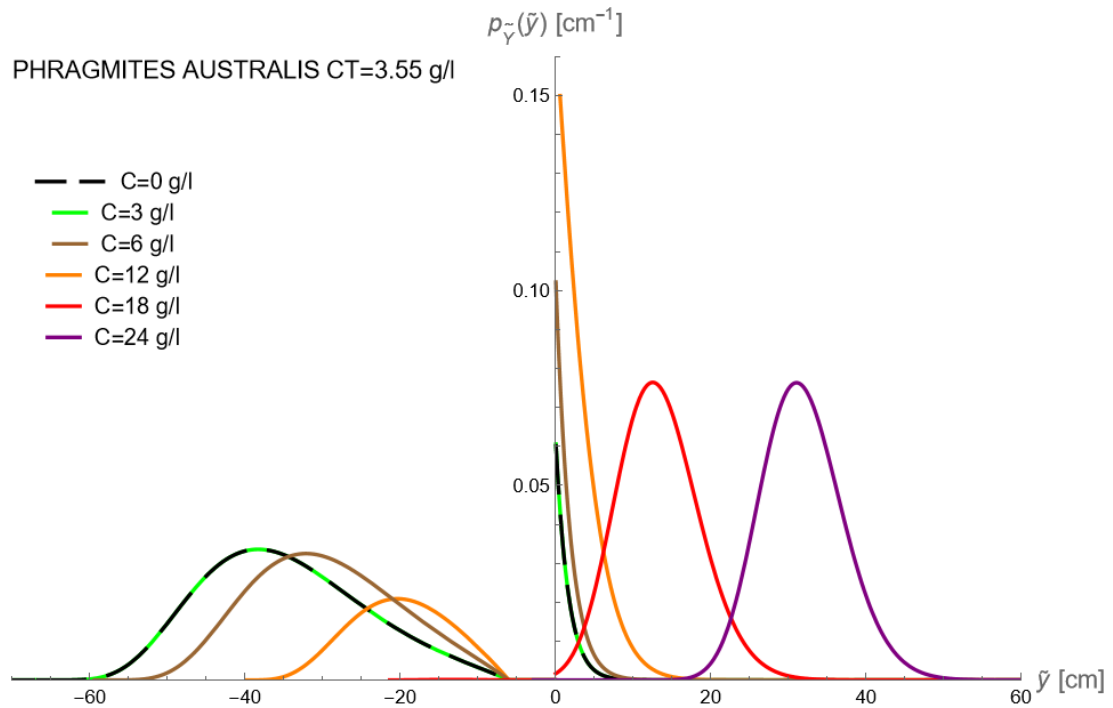


Figure 4.3: Variation of groundwater level PDF in relation to increasing soil salinity concentrations, considering 'Phragmites australis' at a hypothetical site in the Florida Everglades.

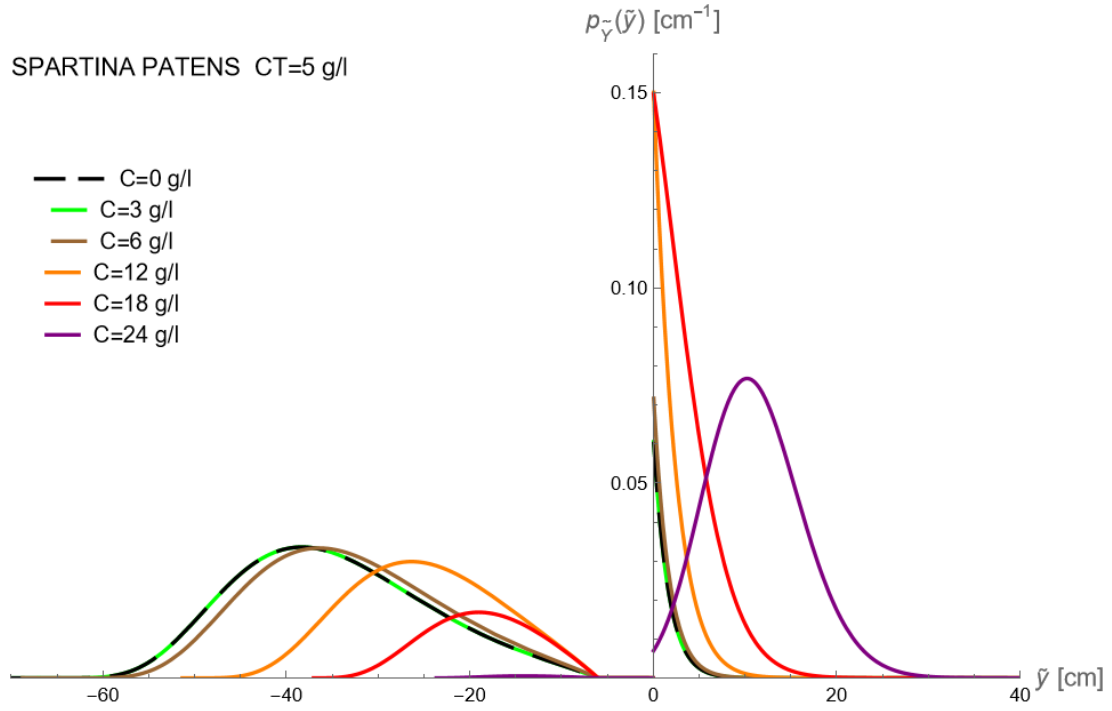


Figure 4.4: Variation of groundwater level PDF in relation to increasing soil salinity concentrations, considering ‘Spartina patens’ at a hypothetical site in the Florida Everglades.

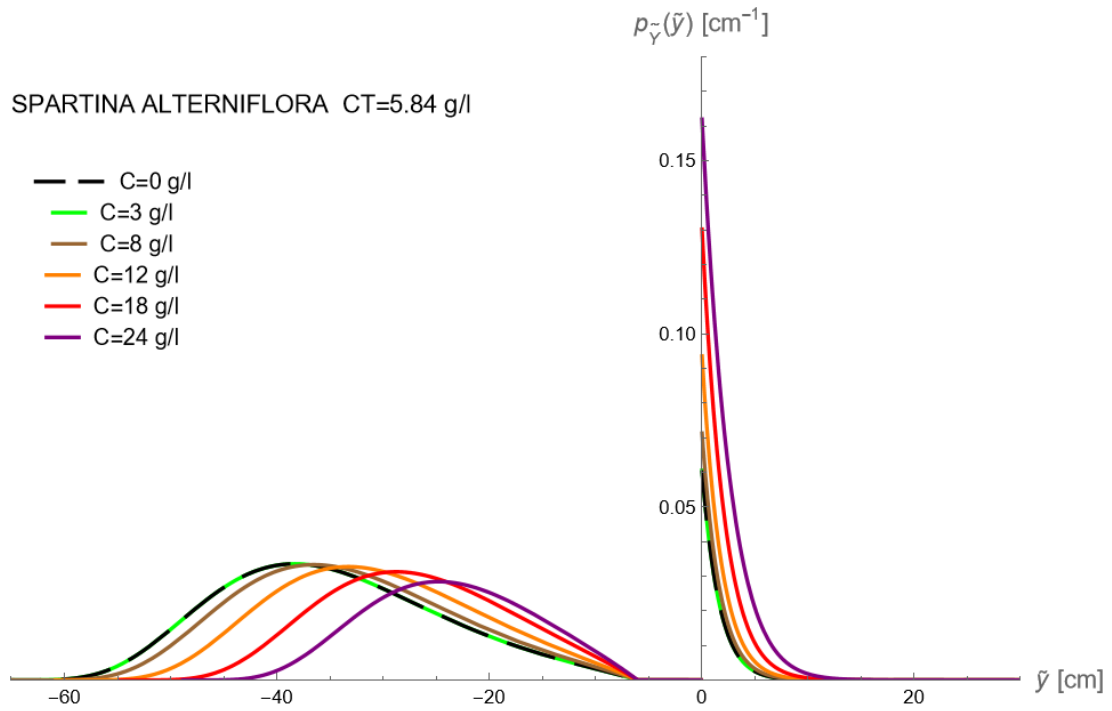


Figure 4.5: Variation of groundwater level PDF in relation to increasing soil salinity concentrations, considering ‘Spartina alterniflora’ at a hypothetical site in the Florida Everglades.

This analysis offers a clear and direct representation of the interaction between vegetation and aquifers in groundwater-dependent ecosystem systems. It highlights how stressful conditions, particularly high salinity, a major factor in coastal wetlands and, in particular, in the Mississippi Delta area, can alter this balance. It is important to note that the modeling is based on steady-state assumptions, assuming a constant value of C over time.

Chapter 5

Analysis and Interpretation of Real In Situ Data

The introduction of salinity and the influence of vegetation provide a preliminary depiction of the water table dynamics in wetland environments. However, the models examined remain predominantly theoretical and, as previously highlighted, are confined to analyzing idealized and equilibrium conditions. This approach overlooks the intrinsic complexity of real-world systems, which are inherently dynamic and influenced by many interrelated factors, such as sea level rise. This discrepancy results in a substantial divergence between the PDFs derived from theoretical models and those obtained from empirical field data. Consequently, the following analysis focuses on evaluating measurements from a site of particular interest, the Birdfoot Delta, specifically highlighting the depth and salinity of the groundwater to assess and interpret the prevailing hydrological conditions.

The data used originate from monitoring stations of the Coastwide Reference Monitoring System (CRMS), whose primary objective is assessing the effectiveness of Louisiana's coastal restoration initiatives. The system operates across multiple spatial scales, ranging from individual project assessments to broader coastal landscape evaluations. With approximately 390 sites spanning various ecological settings, including freshwater, intermediate, brackish, and saline marshes—the CRMS employs standardized protocols for data collection and follows a fixed sampling schedule. These monitoring stations, strategically located within and beyond the areas targeted by restoration and protection projects under the Coastal Wetland Planning, Protec-

tion and Restoration Act (CWPPRA), allow for a comparative analysis of ecological changes between rehabilitated and unrestored regions¹. To ensure accurate measurements, CRMS sites adopt the North American Vertical Datum² of 1988 (NAVD 88) to determine the elevation of land, bodies of water, and other surfaces relative to a common zero point. This datum, established through a levelling network that spans the North American continent—from Alaska and Canada to the United States—is anchored to a single point of origin.

The primary aim is to provide a comprehensive overview of ongoing hydrological dynamics while highlighting inconsistencies between theoretical predictions and observed conditions. In addition, a comparative approach is adopted to improve the interpretation of these processes, incorporating data from other coastal areas of Louisiana. This methodological framework proves particularly valuable, as hydrological data for the region exhibit significant variability and spatial heterogeneity, necessitating a systematic integration of information to ensure reliability and coherence in the findings. However, it is important to note that many monitoring installations within the delta lack piezometers, requiring alternative methodologies for data acquisition. In this context, the term "water level" refers to the height of the water recorded in the nearest hydrological body, measured through level loggers mounted on poles. Similarly, soil salinity concentrations are approximated using salinity values recorded in adjacent water bodies based on the assumption that the saline conditions in surface water serve as a reasonable proxy for those in the surrounding soil. Although these measurements do not directly assess subsurface hydrological conditions, they offer valuable high-resolution data that effectively capture ongoing changes and emerging trends. Refer to Appendix B and Appendix C for further details regarding CRMS instrumentation and data correction methodologies.

5.1 Analysis of NOAA Data on Mean Sea Level Trends at Grand Isle

To begin our analysis, we examined data from the National Oceanic and Atmospheric Administration³ (NOAA), an American agency responsible for monitoring and fore-

¹<https://www.lacoast.gov/crms>

²<https://geodesy.noaa.gov/datums/vertical/north-american-vertical-datum-1988.shtml>

³<https://www.noaa.gov/sites/default/files/2021-10/What-is-NOAA-2011.pdf>

casting changes in Earth’s atmosphere and oceans, as well as overseeing marine resources and protecting endangered species. In this section, we specifically focus on the monthly sea level data recorded at the Grand Isle station in southeast Louisiana at the mouth of Barataria Bay. This data set (different from NAVD88) captures fluctuations in sea level relative to a reference point defined by the Center for Operational Oceanographic Products and Services (CO-OPS), corresponding to the Mean Sea Level (MSL)⁴, which is the region-specific arithmetic mean of hourly sea level heights observed during the period from 1983 to 2001.

Initially, the recorded values are negative, but gradually transition to positive over time. By applying a linear trend to these data, we can project future sea levels and gain valuable insight into regional changes. This analysis thus makes it clear that y_0 , once assumed to be constant, is instead rising steadily, adding complexity to both predictions and our understanding of local groundwater dynamics.

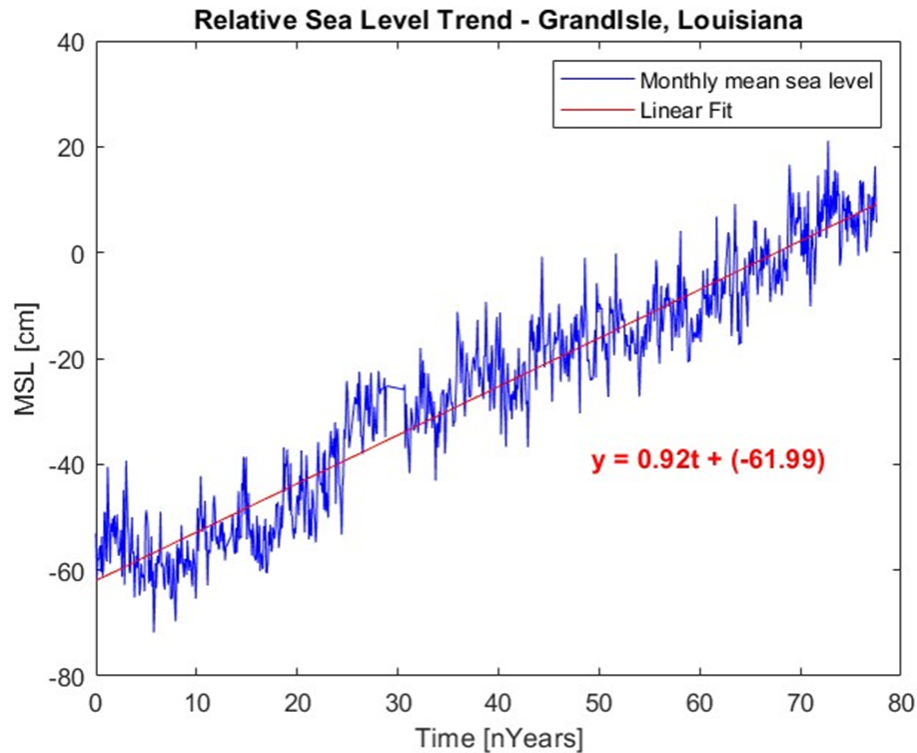


Figure 5.1: Graph of the relative sea level trend at Grand Isle (LA), showing a consistent increase of 0.92 cm per year over an 80-year period. The plot displays the monthly mean sea level measurements (blue line) along with the linear trend (red line).

⁴<https://tidesandcurrents.noaa.gov/datums.html?id=8761724>

5.2 Analysis of Hydrological Conditions in the Birdfoot Area

The focus has now shifted to a more detailed analysis of the stations in the Birdfoot area and the hydrological data collected from them. As shown in Figure 5.3.a, the two dominant plant species in the Birdfoot, *Phragmites australis* and *Sagittaria lancifolia*, have low salt tolerance and show signs of water stress even at moderate salinities. For *Phragmites australis*, maximum relative growth rate (and thus potential transpiration) occurs at relatively low salinity concentrations $CT_{r,max} = 3.55$ ppt. Beyond this threshold, the plant's productivity begins to decline, and the ability of the species to regulate the water table is significantly reduced, even at moderate salinities. The salt thresholds associated with productivity reductions at 40%, 50% and 60% of the maximum (C_{60} , C_{50} , C_{40}) are remarkably low, highlighting the vulnerability of the species even at moderate values. Similarly, *Sagittaria lancifolia* has an even lower $CT_{r,max}$, underlining its greater sensitivity to salt and limited ability to maintain physiological efficiency and influence the water table as salinity increases. Further information on these species can be found in Appendix A. A detailed investigation is carried out for this region, correlating water table depth, sea level, salinity concentrations and their temporal variations. A four-year moving average was applied to these parameters to better understand their temporal evolution and local conditions. However, it is important to recognize that human activities, such as the construction and abandonment of artificial channels for gas extraction, have profoundly affected the landscape and natural water flow in the region, influencing the hydrological data collected and complicating their interpretation. Therefore, a classification system was employed to account for the specific locations of the analyzed sites. CRMS stations located inland are primarily influenced by the Mississippi River system and thus are categorized as "river-dominated" zones. In contrast, stations located on the outer edges of the delta, closer to the sea, are more affected by oceanic dynamics, and so are classified as "ocean-dominated" (Figure 5.2).

In Figure 5.3.b, temporal changes in salinity among the observed stations consistently remain below the critical threshold for the dominant species in the region. However, notable peaks, particularly around 2013 and more recently, were observed, likely corresponding to drought periods. This pattern is especially evident at sites with more significant oceanic influence, such as CRMS 4626, where higher salinity concentrations are recorded due to increased exposure to marine conditions. Con-

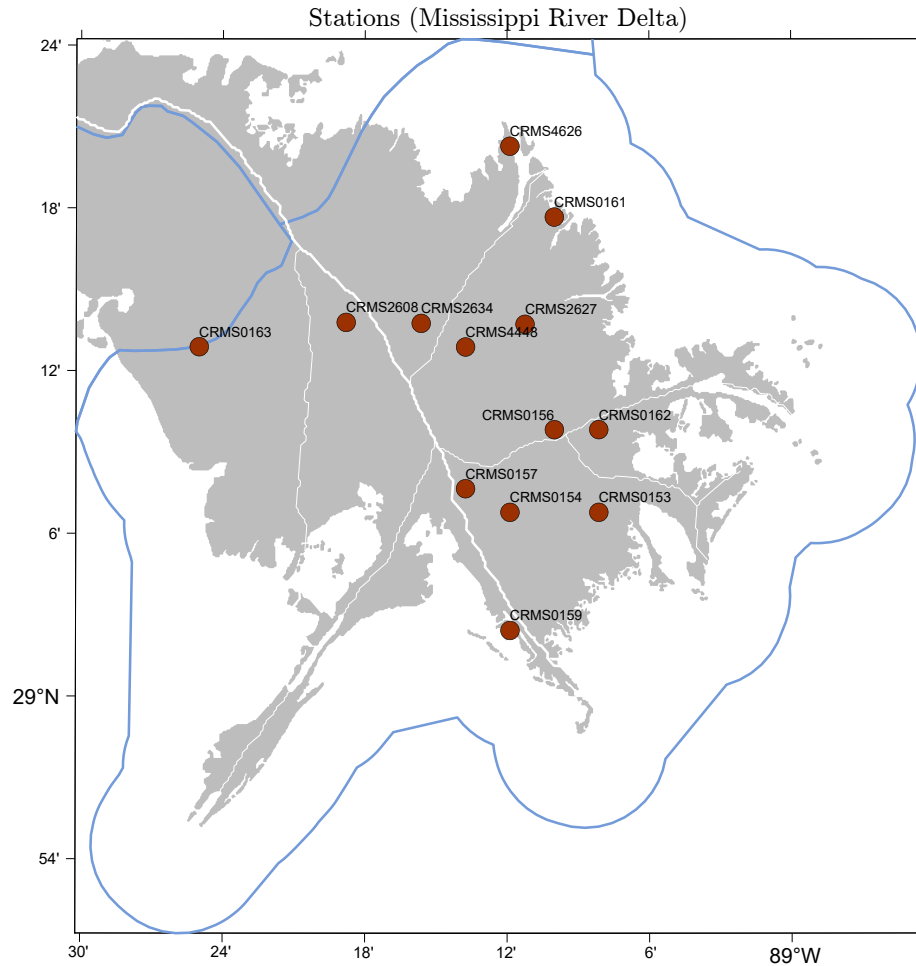


Figure 5.2: Spatial visualization of the various CRMS sites within the modern MRD.

versely, inland sites, which are more influenced by river water, exhibit lower salinity values with less pronounced fluctuations. Regarding the variation in water table depth over time (Figure 5.3.c), a general upward trend is evident across all stations, though periodic reductions, often linked to drought conditions, are also apparent. A significant positive peak in water table depth was recorded at more central points, such as CRMS 2634, in 2020. This event may be associated with an increase in Mississippi River flow, likely driving a rise in water table levels and highlighting the pivotal role of river dynamics in local hydrological processes. Examining the relationship between the depth of the aquifer and the sea level (see Figure 5.3.d), a clear linear correlation emerges, indicating how fluctuations in sea level have a strong impact and influence on the aquifer. This finding is significant, suggesting that vegetation in the monitored areas cannot effectively regulate groundwater depth despite the relatively low salinity levels recorded. Furthermore, it is important to note that stations closer to the ocean,

such as CRMS 0159, tend to have lower water table levels than inland stations like CRMS 2634. This difference is evident in the temporal analysis and the relationship with sea-level variations. The influence of the river, particularly in the northern part of the delta, helps maintain higher water table levels inland, in contrast to the oceanic forces dominating more coastal areas. Figure 5.3.e illustrates the temporal variation in the difference (Δy) between water table depth and sea level, with the trend in this parameter closely reflecting the changes observed in groundwater depth over time. In coastal stations such as CRMS 0159, Δy remains positive, indicating that the water table is consistently below sea level, primarily due to the diminished effect of river dynamics in these areas. Notably, a negative peak in Δy occurred around 2020, attributed to a surge in river influence during that period. Furthermore, as previously highlighted, the temporal analysis of y_0 (Figure 5.3.f) reveals a generally upward trend (dashed orange line) with only minor fluctuations, which further supports the observed patterns in groundwater dynamics. In the presented graph, the Annual Sea Level (orange points) represents the measured annual mean value, while the 4-Year Moving Average (purple points) corresponds to the mean value computed over the preceding four years.

To better understand the hydrological conditions in the study area, a more detailed examination is proposed to study the ranges of variation in both water level and salinity for each station over a given period, along with the corresponding probability densities. However, for the sake of brevity, we focus on two representative sites: one dominated by oceanic influences (CRMS 0163) and one by the river system (CRMS 2608). This approach provides a comprehensive and balanced perspective on the hydrological dynamics of the region, and additional information on conditions at other MRD stations can be found in the Appendix D.

The CRMS 0163 station, located in the north-western part of the Birdfoot area and mainly influenced by oceanic factors, shows moderate fluctuations in groundwater depth over the observation period, considering its annual variation. The water table generally remains below the land surface, limiting flooding events. This is also due to a steady, albeit moderate, increase in surface elevation, which stabilizes in the last two years of observation. Furthermore, in 2024, the water table not only remains well below the surface but also shows a decreasing trend, indicating a current drought condition in the area (Figure 5.4.a). These comments are supported by the histogram in the top right-hand corner (Figure 5.4.b), which shows a left-skewed unimodal

Mississippi River Delta

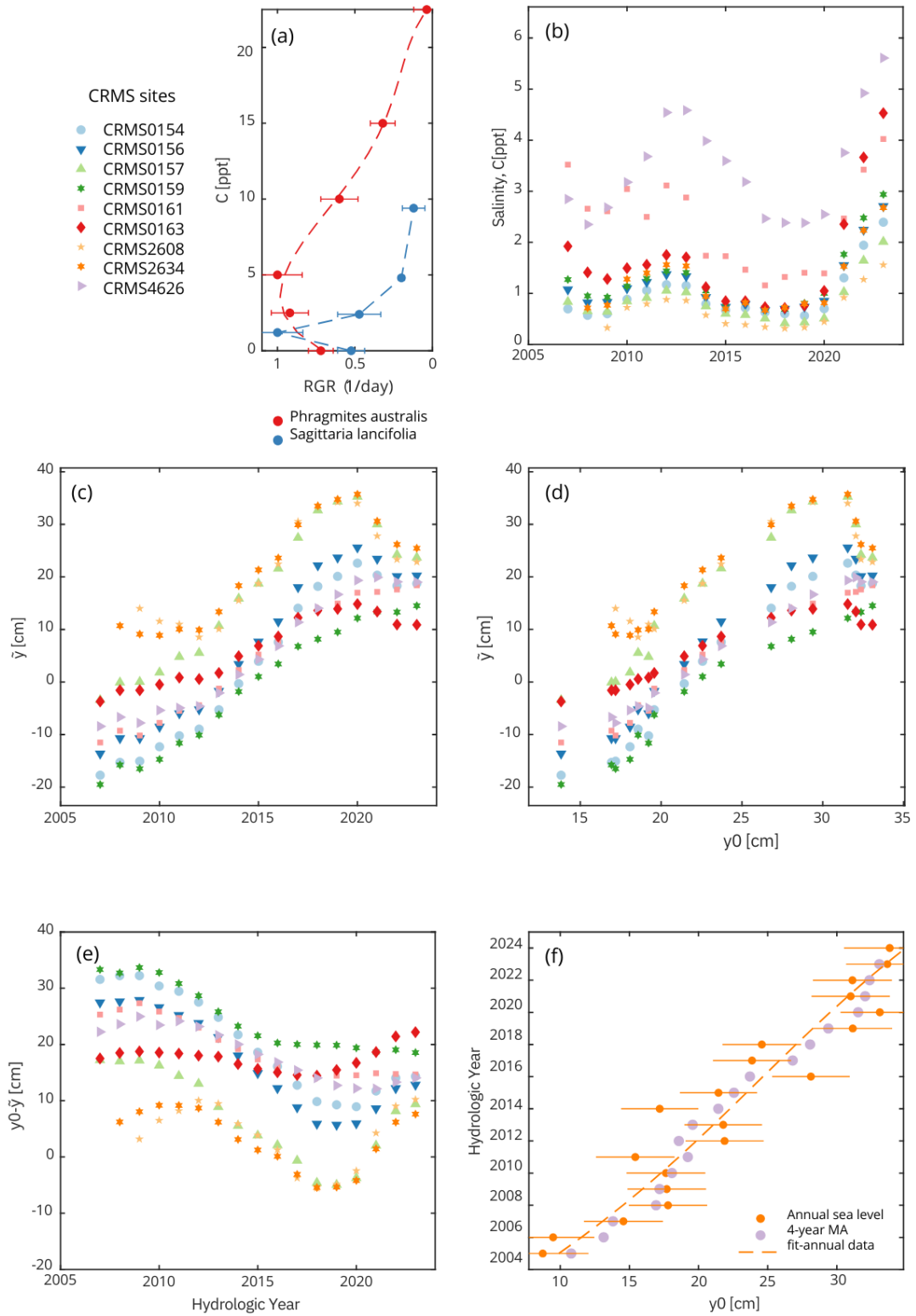


Figure 5.3: Observed relationships between key hydrological parameters and their evolution over time for the various CRMS stations in the MRD.

distribution. The peak of the distribution is centered around 0, while the left tail extends down to -40 cm and is more pronounced compared to the right tail, which decreases rapidly for values above about 20 cm. This pattern suggests a predominance of SWT conditions over flooding.

Regarding trends in salinity over time (Figure 5.4.c), daily fluctuations exhibit significant oscillations and multiple peaks, likely due to natural factors such as tides, precipitation, saltwater intrusion, or seasonal shifts. However, the annual averages show less variability, suggesting an overall decrease in salt concentrations between 2014 and 2018, followed by a gradual rebound, reaching its highest point in 2024. This pattern aligns with previous observations, as the drop in the water table—indicating drought conditions—corresponds with an increase in salinity. Notably, in 2020, the lowest values were recorded, likely due to a substantial influx of freshwater from the river that reduced seawater intrusion. The histogram of concentration levels (Figure 5.4.d) mirrors these low values, presenting a positively skewed distribution with a peak near zero concentrations.

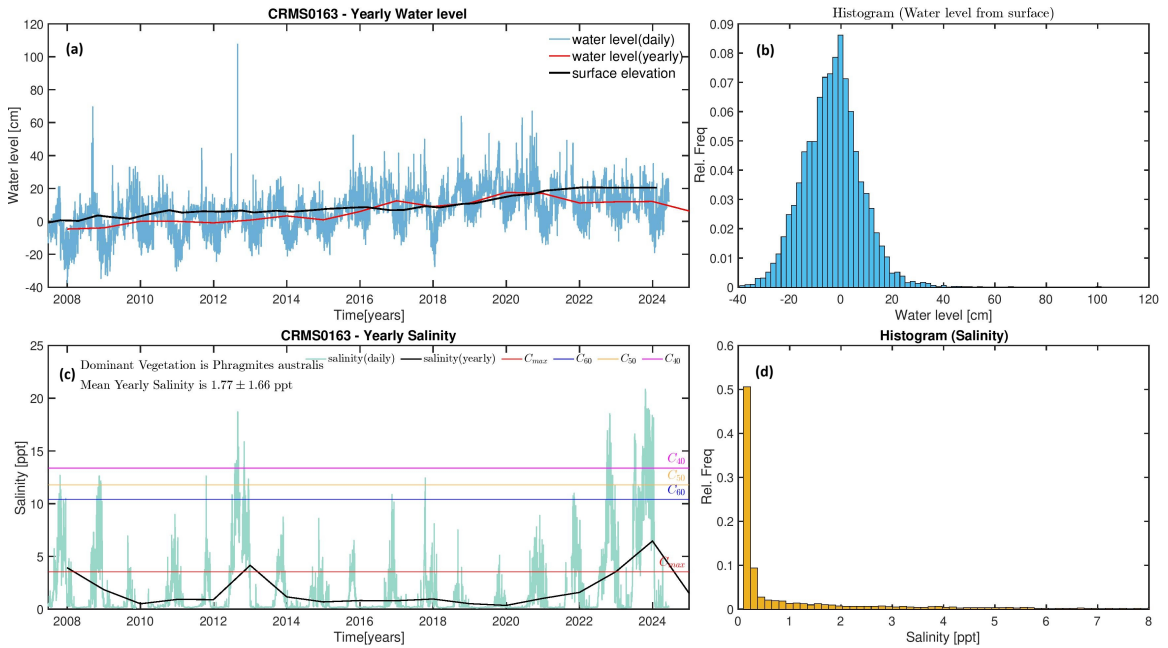


Figure 5.4: Temporal variations in the water table and salinity at CRMS 0163, along with their corresponding probability histograms.

On the other hand, the CRMS 2608 station is situated in a river-dominated area near the Mississippi River, in the central-northern part of the delta. As depicted in Figure 5.5.a, the annual water table trend in this region demonstrates greater fluctuation.

tuation relative to the previous site, with three distinct phases identifiable in the evolution of the hydrological system. The first one, spanning roughly from 2010 to 2015, is characterized by modest oscillations, with the water table generally remaining below the surface. Between 2016 and 2020, there was a progressive rise in water levels, reaching a peak in 2020, linked to increased river flow. From 2021 to 2024, the system stabilizes, showing a slight decline with the water table approaching the surface. Surface elevation gradually increases over time, followed by stabilization in recent years. These observations are corroborated by the water table histogram shown in Figure 5.5.b, which reveals a bimodal, asymmetrical distribution, predominantly shifted toward positive water table values, with values surpassing 50 cm. This suggests a prevalence of flooding conditions over SWT conditions, reinforcing the river’s dominant influence on the area’s hydrological regime. Regarding saltiness, the annual trend remains extremely low between 2014 and 2020, often near zero. However, salinity peaks were recorded in 2013 and 2024, corresponding with drought episodes, which are consistent with lower water table levels, as shown in Figure 5.5.c. The salinity histogram (Figure 5.5.d) exhibits a markedly asymmetrical distribution, with a dominant peak between 0 and 1 ppt, indicating the predominance of freshwater or low-concentration conditions. Furthermore, the steep decline in frequency with increasing C values suggests that occurrences of elevated salinity are improbable.

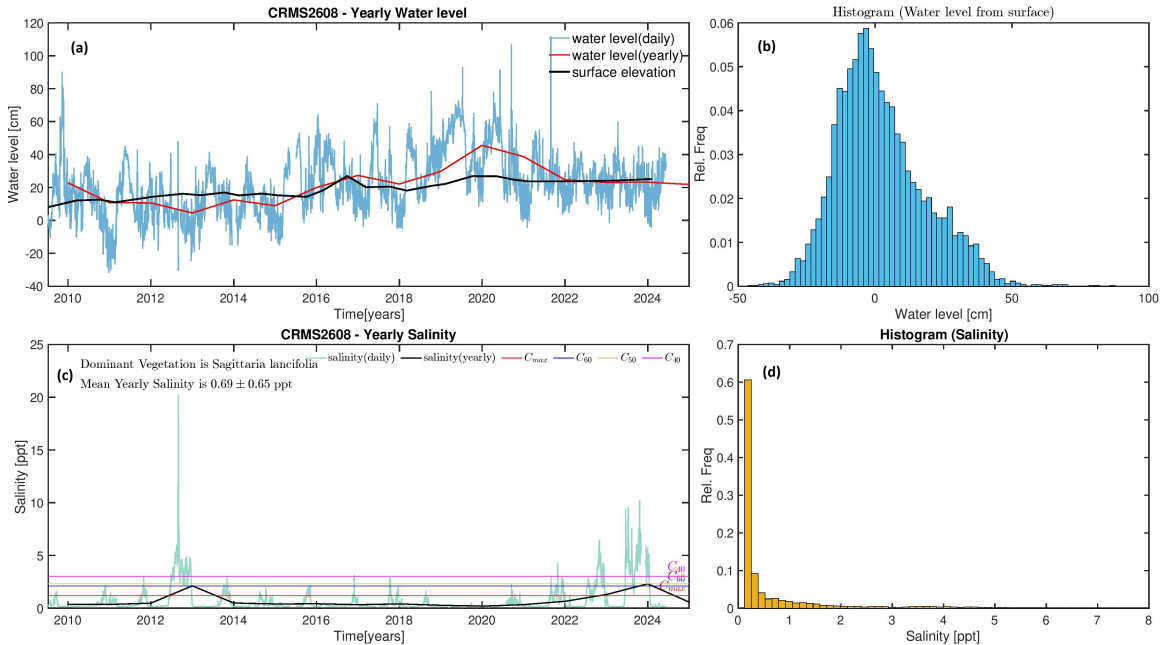


Figure 5.5: Temporal variations in the water table and salinity at CRMS 2608, along with their corresponding probability histograms.

5.3 Comparative Overview of Hydrological Conditions in the Terrebonne Basin

The second basin analyzed, known as the Terrebonne Basin⁵, was included to broaden the understanding of the hydrological characteristics of coastal wetlands in this region. This abandoned delta complex comprises about 627,285 km^2 of wetlands and nearly 2,323.02 km^2 of marshes, ranging from freshwater marshes in the interior to brackish and saline marshes near the bays and gulf. The area is characterized by thick layers of unconsolidated sediments prone to dewatering and compaction, leading to significant subsidence, and a network of ancient distributary dikes.

One distinctive characteristic of this area is the diversity of the predominant plant species, many of which have a limited or moderate tolerance to salinity (Figure 5.6.a). The analysis of the temporal distribution of salinity levels, illustrated in Figure 5.6.b, reveals considerable variability between the different monitoring locations. The areas closer to the ocean show a higher average salinity than the more inland sites, such as CRMS 4045, where values remain around one ppt. In contrast, at CRMS 0292, salinity levels reach 25 ppt, significantly exceeding those recorded in the Balize Delta. Although fluctuations can be identified due to climatic phenomena, such as droughts or increased river inputs, these variations appear less pronounced than those observed in the previous basin. The water table shows an upward temporal trend, mirroring the pattern observed in the MRD, with values influenced by seasonal fluctuations and broader hydrological dynamics (Figure 5.6.c). This trend is also supported by the temporal evolution of Δy , as shown in Figure 5.6.e. Notably, a linear correlation between the variables y_0 and y re-emerges (Figure 5.6.d), highlighting, much like in the Birdfoot region, the strong influence of rising sea levels on the water table, that is further depicted in Figure 5.6.f.

For a more detailed analysis, individual monitoring stations were carefully examined, and among them, CRMS 0292 stands out as a site significantly affected by salinization. This station serves as a representative case, as many other sites within the basin, as illustrated in Figure 5.6.b, exhibit similarly elevated salinity levels. Throughout the observation period, the groundwater level remained consistently just below the soil surface (Figure 5.7.a), although a slight uplift, ranging from 0 to 20 cm, was recorded over time. However, this change was accompanied by a con-

⁵https://lacoast.gov/new/about/Basin_data/te/Default.aspx

Terrebonne

CRMS sites

- CRMS0292
- ▼ CRMS0293
- ▲ CRMS0303
- ★ CRMS0305
- ◆ CRMS0307
- ◇ CRMS0309
- ☆ CRMS0310
- ✦ CRMS0311
- ✧ CRMS0315
- ✪ CRMS0318
- ✫ CRMS0319
- ✬ CRMS0322
- ✭ CRMS0326
- ✮ CRMS0332
- ✯ CRMS0335
- ✰ CRMS0336
- ✱ CRMS0337
- ✲ CRMS0338
- ✳ CRMS0345
- ✴ CRMS0347
- ✵ CRMS0354
- ✶ CRMS0355
- ✷ CRMS0369
- ✸ CRMS0374
- ✹ CRMS0377
- ✺ CRMS0383
- ✻ CRMS0386
- ✼ CRMS0390
- ✽ CRMS0392
- ✾ CRMS0394
- ✿ CRMS0395
- ⬠ CRMS0396
- ⬡ CRMS0397
- ⬣ CRMS0398
- ⬤ CRMS0399
- ⬥ CRMS0400
- ⬦ CRMS0416
- ⬧ CRMS0421
- ⬨ CRMS0978
- ⬩ CRMS2825
- ⬪ CRMS4045

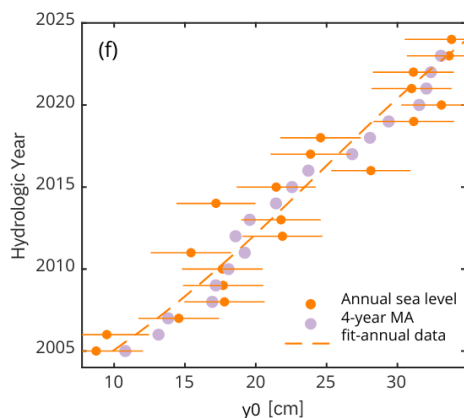
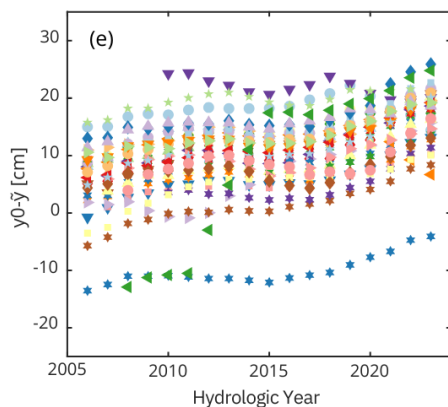
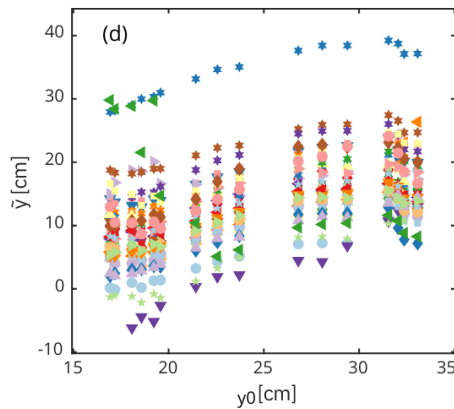
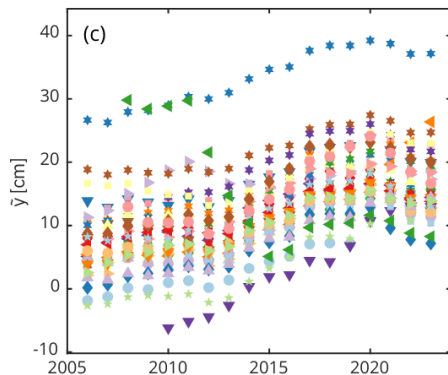
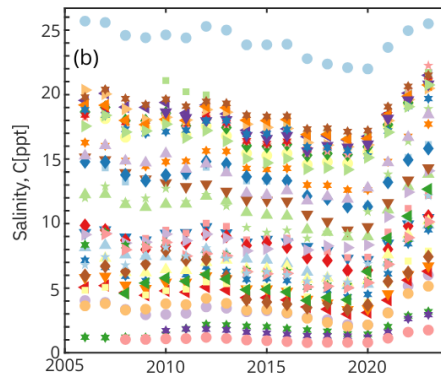
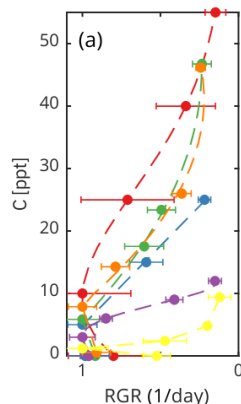


Figure 5.6: Observed relationships between key hydrological parameters and their temporal evolution across different CRMS stations in the Terrebonne Basin.

current increase in surface altitude, leading to a shift in the associated histogram towards below-ground values (Figure 5.7.b). This pattern underscores the predominance of SWT conditions over the WL period, thereby highlighting the critical role of surface elevation dynamics in interpreting the data. Concerning salinity, in-situ measurements consistently indicate persistently high values that exceed the maximum tolerance threshold ($CT_{r,max}$) for the dominant vegetation species, *Avicennia germinans* (Figure 5.7.c). The related histogram corroborates this finding, revealing a higher probability of elevated C levels (Figure 5.7.d). While proximity to the ocean undoubtedly represents a primary driver of these conditions, it is also plausible that nearby anthropogenic infrastructure exerts an additional influence. These results suggest that local vegetation is subjected to intense environmental stress, leading to a drastic, if not complete, reduction in its capacity to influence groundwater dynamics, rendering groundwater fluctuations closely dependent on sea-level variations.

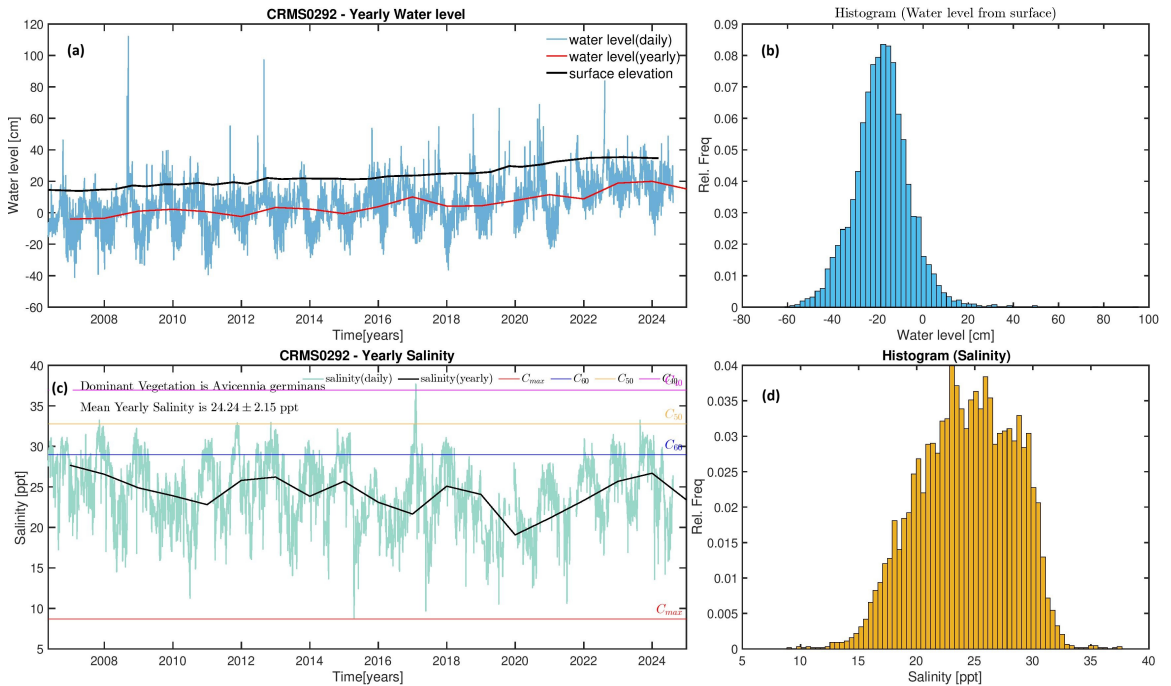


Figure 5.7: Temporal variations in the water table and salinity at CRMS 0292, along with their corresponding probability histograms.

Some of the innermost sites, however, exhibit different dynamics, as in the case of CRMS 0354, where both groundwater fluctuations and surface elevation changes are minimal, suggesting that the system has maintained a stable state throughout the entire analysis period (Figure 5.8.a). Moreover, the water table level remains consistently near the surface, as evidenced by the histogram in Figure 5.8.b, which displays

a symmetrical unimodal distribution with a well-defined peak around zero, indicating that groundwater levels are predominantly concentrated near the soil surface. This pattern is associated with more moderate salinity levels than the previously analyzed site. Although the average annual salinity exhibits fluctuations, it remains predominantly below the critical threshold, with concentration peaks surpassing this limit only around 2007 and 2024, whereas a minimum is recorded in 2020, likely due to phenomena similar to those already described in the MRD analysis (Figure 5.8.c). Furthermore, the salinity histogram reveals a positively skewed distribution, with most values ranging between 0 and 5 ppt. However, the recent rise in salinity could account for the extended right-hand tail of the histogram, where values exceed 20 ppt (Figure 5.8.d).

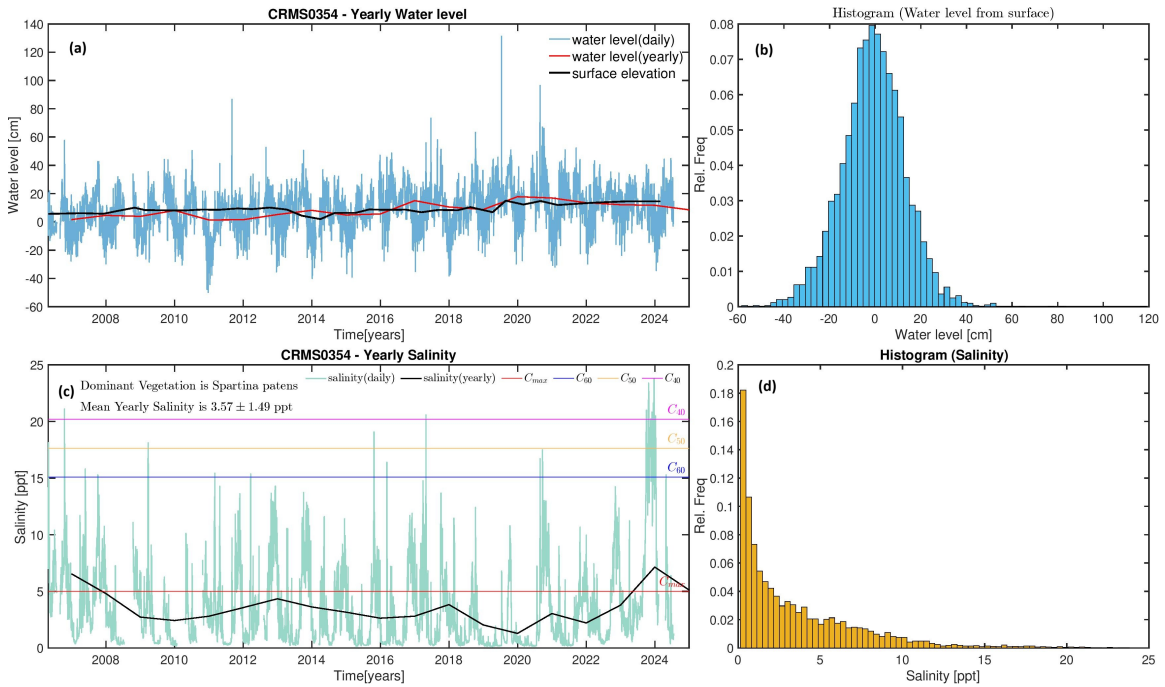


Figure 5.8: Temporal variations in the water table and salinity at CRMS 0354, along with their corresponding probability histograms.

The analysis highlights how the dynamic variation of the groundwater table is closely linked to a complex interaction of interdependent factors. Among these, the influence of river and oceanic regimes, temporal fluctuations in the elevation of the marsh surface, and other site-specific dynamics are particularly significant. The difficulty in precisely identifying the causes of the observed variations arises from the complexity and number of the elements involved. Furthermore, discrepancies between theoretical predictions and the actual conditions encountered suggest the need

to update and refine the proposed models, integrating a greater number of factors influencing the aquifer and, in particular, their temporal variation. This would allow for overcoming a static analysis, promoting a dynamic representation over time that can fully capture the complexity of the systems in question.

Chapter 6

Conclusions

The analysis of dynamic water table variation in coastal wetlands is a critical topic given these environments' numerous ecosystem and economic services. A detailed understanding of the various mechanisms at play and future predictions of the trends in hydrological variables is essential to protecting these extremely vulnerable habitats, particularly the modern Mississippi River delta, where the highest rates of soil loss occur worldwide. Therefore, in recent years, considerable interest has been shown in proposing stochastic models that study how groundwater levels vary in the GDEs, which is essential for the ecosystem's well-being and survival. The first approach investigated assumes an ideal soil column and considers the possibility of waterlogging. However, it neglects the stressful effect that salinity has on vegetation transpiration and, consequently, on its control of the water table. Despite this, there is still a certain similarity between the PDFs modeled by numerical or analytical resolution and those derived from empirical data, despite several simplifying assumptions at the basis and the approximation of some input parameters. Regardless of the type of resolution used, the model is a useful and, on the whole, reliable tool for studying aquifer-level variability in these domains. However, one must consider that this concordance, although present for the cases analyzed, is strongly linked to the choice of site to be examined.

Indeed, in regions where salinity is not negligible, it is necessary to go a step further and consider the reduction in plant transpiration as salt concentration increases. Further modeling has been re-proposed using analytical resolution only. This consideration makes the conditions more similar to those found in the Birdfoot area,

where average salinity is not high but can exceed $CT_{r,max}$ of the species present during drought years. However, the limited availability of rainfall and soil hydraulics data at the delta CRMS stations necessitated the use of a set of input values to the model describing a hypothetical site in the Everglades, assuming a similarity with the characteristics of the MRD. Species characteristic of the Balize delta were used to show their tolerance to saline conditions regarding water table control and allow for comparison. The solutions obtained clearly show the effect of salt stress on the different species in terms of changes in the water table pdf, with a shift in the area subtended by the curves towards positive values of \tilde{y} , emphasizing the greater tendency of the soil surface to flood. What emerges is the interesting interconnection between salinity-vegetation and water table dynamics.

However, it should be emphasized that the considered modeling framework focuses on the steady-state conditions, i.e., a state of equilibrium that the ecosystem reaches over extended periods in which the water table level remains, on average, around a specific value over time and neglects the temporal variation of key processes like salt-water intrusion and sea level. Therefore, in actual conditions, the situation of the Birdfoot is much more complex and highly heterogeneous, and there are numerous elements to consider. First of all, the sea level is increasing over time, as does the surface elevation, and these factors are a function of the site's location. The Mississippi River is a pivotal actor in local hydrology, as its flow variations affect the water table level, and the constant sediment supply plays an essential role in the area's configuration. The intense human impact on the region has also been analyzed, with, for example, the construction of artificial canals for the oil and gas industry, the creation of dams for greater control of the river's flow, and the extraction of fuels altering the local hydrology and accelerating the rate of subsidence.

All these facets are strongly interconnected, posing a significant threat to the future of these ecosystems – and the MRD in particular. Based on the considerations made and the limitations of the approaches highlighted, a helpful next step could be creating a numerical model based on the simulation of many possible water table trajectories over time by implementing a so-called Marked Poisson Process. However, the starting point remains the soil water balance, and the different trajectories will vary as a stochastic precipitation input is considered. This would make it possible to integrate into the modeling a more significant amount of key drivers influencing the aquifer, but above all, to consider the variation over time of parameters hitherto

regarded as constant, such as sea level or salinity, making it possible to move away from a simple probabilistic steady-state treatment and instead to grasp the temporal dynamics of these processes. This would then coincide with having probability distributions varying in time, thus having a more faithful representation of the conditions in situ. The future of coastal wetlands, hence, depends on our ability to embrace and model the complexity of their environmental processes.

Chapter 7

Code availability

The Wolfram Mathematica codes used to simulate the stochastic water table dynamics in coastal wetlands are available at <https://github.com/RiccardoDellaCorte/Code-wolfram-water-table-models->

Bibliography

- Acosta-Motos JR, Ortuño MF, Bernal-Vicente A, Diaz-Vivancos P, Sanchez-Blanco MJ, Hernandez JA (2017) Plant responses to salt stress: adaptive mechanisms. *Agronomy* 7(1):18
- Cahoon D, Lynch J, Perez B, Segura B, Holland R, Stelly C, Stephenson G, Hensel P (2002) High-precision measurements of wetland sediment elevation: Ii. the rod surface elevation table. *Journal of Sedimentary Research - J SEDIMENT RES* 72:734–739, DOI 10.1306/020702720734
- Clark WR, Clay RT (1985) Standing crop of sagittaria in the upper mississippi river. *Canadian journal of botany* 63(8):1453–1457
- Coleman J SG Roberts H (1998) Mississippi river delta: An overview
- Costanza R, Pérez-Maqueo O, Martinez ML, Sutton P, Anderson SJ, Mulder K (2008) The value of coastal wetlands for hurricane protection. *Ambio* pp 241–248
- Couvillion BR, Beck H, Schoolmaster D, Fischer M (2017) Land area change in coastal louisiana (1932 to 2016). Tech. rep., US Geological Survey
- Davis D, Guidry R (1996) Oil, oil spills and the state's responsibilities. *Basin Res Inst Bull* 6:60–68
- Day JW, Christian RR, Boesch DM, Yáñez-Arancibia A, Morris J, Twilley RR, Naylor L, Schaffner L, Stevenson C (2008) Consequences of climate change on the ecogeomorphology of coastal wetlands. *Estuaries and coasts* 31:477–491
- Day JW, Clark HC, Chang C, Hunter R, Norman CR (2020) Life cycle of oil and gas fields in the mississippi river delta: A review. *Water (Switzerland)* 12, DOI 10.3390/w12051492

- Day JW, Xu YJ, Keim BD, Brown VM, Giosan L, Mann ME, Stephens JR (2024) Emerging climate threats to the mississippi river delta: Moving from restoration to adaptation. DOI 10.1016/j.oneear.2024.03.001
- Engle VD (2011) Estimating the provision of ecosystem services by gulf of mexico coastal wetlands. *Wetlands* 31(1):179–193
- Folse TM, Sharp LA, West JL, Hymel MK, Troutman JP, McGinnis TE, Weifenbach D, Boshart WM, Rodrigue LB, Richardi DC, Wood WB, Miller CM (2018) A standard operating procedures manual for the coastwide reference monitoring system-wetlands
- Hao Q, Song Z, Zhang X, He D, Guo L, van Zwieten L, Yu C, Wang Y, Wang W, Fang Y, et al. (2024) Organic blue carbon sequestration in vegetated coastal wetlands: Processes and influencing factors. *Earth-Science Reviews* p 104853
- Heinrich P, Paulsell R, Milner R, Snead J, Peele H (2015) Investigation and gis development of the buried holocene-pleistocene surface in the louisiana coastal plain
- Heliotis FD, DeWitt CB (1987) Rapid water table responses to rainfall in a northern peatland ecosystem 1. *JAWRA Journal of the American Water Resources Association* 23(6):1011–1016
- Huang Y, Sun W, Zhang W, Yu Y, Su Y, Song C (2010) Marshland conversion to cropland in northeast china from 1950 to 2000 reduced the greenhouse effect. *Global Change Biology* 16(2):680–695
- Kar SK, Nema A, Singh A, Sinha B, Mishra C (2016) Comparative study of reference evapotranspiration estimation methods including artificial neural network for dry sub-humid agro-ecological region. *Journal of Soil and Water Conservation* 15(3):233–241
- Kirwan ML, Megonigal JP (2013) Tidal wetland stability in the face of human impacts and sea-level rise. *Nature* 504(7478):53–60
- Kolker AS, Allison MA, Hameed S (2011) An evaluation of subsidence rates and sea-level variability in the northern gulf of mexico. *Geophysical Research Letters* 38(21)

- Laio F, Tamea S, Ridolfi L, D'Odorico P, Rodriguez-Iturbe I (2009) Ecohydrology of groundwater-dependent ecosystems: 1. stochastic water table dynamics. *Water Resources Research* 45, DOI 10.1029/2008WR007292
- Li G, Törnqvist TE, Dangendorf S (2024) Real-world time-travel experiment shows ecosystem collapse due to anthropogenic climate change. *Nature Communications* 15, DOI 10.1038/s41467-024-45487-6
- Li X, Bellerby R, Craft C, Widney SE (2018) Coastal wetland loss, consequences, and challenges for restoration. *Anthropocene Coasts* 1(1):1–15
- Macreadie PI, Anton A, Raven JA, Beaumont N, Connolly RM, Friess DA, Kelleway JJ, Kennedy H, Kuwae T, Lavery PS, et al. (2019) The future of blue carbon science. *Nature communications* 10(1):1–13
- Marburger JE (1993) Biology and management of *sagittaria latifolia* willd (broad-leaf arrow-head) for wetland restoration and creation. *Restoration ecology* 1(4):248–255
- McKee KL, Mendelssohn IA (1989) Response of a freshwater marsh plant community to increased salinity and increased water level. *Aquatic Botany* 34(4):301–316
- Mclaughlin D, Cohen M (2014) Ecosystem specific yield for estimating evapotranspiration and groundwater exchange from diel surface water variation. *Hydrological Processes* 28, DOI 10.1002/hyp.9672
- Milke J, Gałczyńska M, Wróbel J (2020) The importance of biological and ecological properties of *phragmites australis* (cav.) trin. ex steud., in phytoremediation of aquatic ecosystems—the review. *Water* 12(6), URL <https://www.mdpi.com/2073-4441/12/6/1770>
- Moore KA, Fisher LE, Della Torre CJ, Gettys LA (2016) Native aquatic and wetland plants: Duck potato, *sagittaria lancifolia*: Ss-agr-399/ag403, 12/2015. *EDIS* 2016(1):3–3
- Nobel PS (1983) *Biophysical plant physiology and ecology*.
- Olson KR, Suski CD (2021) Mississippi river delta: Land subsidence and coastal erosion. *Open Journal of Soil Science* 11:139–163, DOI 10.4236/ojss.2021.113008
- Parida AK, Das AB (2005) Salt tolerance and salinity effects on plants: a review. *Ecotoxicology and environmental safety* 60(3):324–349

- Perri S, Entekhabi D, Molini A (2018) Plant osmoregulation as an emergent water-saving adaptation. *Water Resources Research* 54:2781–2798, DOI 10.1002/2017WR022319, URL <https://agupubs.onlinelibrary.wiley.com/doi/10.1002/2017WR022319>
- Perri S, Krauss KW, Molini A (Under Review) Coastal salinization drives irreversible hydrological change in tidal wetlands
- Polash MAS, Sakil M, Hossain MA (2019) Plants responses and their physiological and biochemical defense mechanisms against salinity: A review DOI 10.22271/tpr.2019.v6.i2.035
- Pumo D, Tamea S, Noto LV, Miralles-Wilhem F, Rodriguez-Iturbe I (2010) Modeling belowground water table fluctuations in the everglades. *Water Resources Research* 46, DOI 10.1029/2009WR008911
- Reed DJ (1995) The response of coastal marshes to sea-level rise: Survival or submergence? *Earth Surface processes and landforms* 20(1):39–48
- Ridolfi L, D’Odorico P, Laio F, Tamea S, Rodriguez-Iturbe I (2008) Coupled stochastic dynamics of water table and soil moisture in bare soil conditions. *Water resources research* 44(1)
- Roberts HH (1997) Dynamic changes of the holocene mississippi river delta plain: the delta cycle. *Journal of Coastal Research* pp 605–627
- Saltonstall K (2003) Microsatellite variation within and among north american lineages of *phragmites australis*. *Molecular Ecology* 12(7):1689–1702
- Scott DB, Frail-Gauthier J, Mudie PJ, Mudie PJ (2014) Coastal wetlands of the world: geology, ecology, distribution and applications. Cambridge University Press
- Skaggs T, Anderson R, Corwin D, Suarez D (2014) Analytical steady-state solutions for water-limited cropping systems using saline irrigation water. *Water Resources Research* 50(12):9656–9674
- Suedel BC, McQueen AD, Wilkens JL, Saltus CL, Bourne SG, Gailani JZ, King JK, Corbino JM (2021) Beneficial use of dredged sediment as a sustainable practice for restoring coastal marsh habitat. *Integrated Environmental Assessment and Management* 18(5):1162–1173

- Tamea S, Laio F, Ridolfi L, D'Odorico P, Rodriguez-Iturbe I (2009) Ecohydrology of groundwater-dependent ecosystems: 2. stochastic soil moisture dynamics. *Water Resources Research* 45, DOI 10.1029/2008WR007293
- Tamea S, Muneeppeerakul R, Laio F, Ridolfi L, Rodriguez-Iturbe I (2010) Stochastic description of water table fluctuations in wetlands. *Geophysical Research Letters* 37, DOI 10.1029/2009GL041633
- Van Huyssteen CW (2023) Wetland soils. In: Goss MJ, Oliver M (eds) *Encyclopedia of Soils in the Environment (Second Edition)*, second edition edn, Academic Press, Oxford, pp 436–446, DOI <https://doi.org/10.1016/B978-0-12-822974-3.00064-1>, URL <https://www.sciencedirect.com/science/article/pii/B9780128229743000641>
- Vasquez EA, Glenn EP, Guntenspergen GR, Brown JJ, Nelson SG (2006) Salt tolerance and osmotic adjustment of *spartina alterniflora* (poaceae) and the invasive haplotype of *phragmites australis* (poaceae) along a salinity gradient. *American Journal of Botany* 93(12):1784–1790
- Youssef RB, Boukari N, Abdelly C, Jelali N (2023) Salicylic acid phytohormone as a new potential for adaptation and improvement of metabolic responses of fodder species under separate and combined impact of salinity and fe deficiency constraints. In: *Phytohormones and Stress Responsive Secondary Metabolites*, Elsevier, pp 249–263
- Zhao Q, Bai J, Huang L, Gu B, Lu Q, Gao Z (2016) A review of methodologies and success indicators for coastal wetland restoration. *Ecological indicators* 60:442–452

Appendix A

Dominant Vegetation in the Birdfoot

The following appendix describes the main characteristics of the prevalent species in the Balize delta, without, however, going into a detailed discussion of the various aspects of these plants.

The first species considered is the "Phragmites australis" (Common reed), a perennial reed characteristic of wetlands that can adapt to fresh and saltwater conditions [Saltonstall (2003)]. The name is given by its shape, which has cane-like stems that can reach more than 4.6 m in height. The foliage is characterized by broad, pointed (glabrous) leaves ranging from 15 to 60 cm in length¹. The root system develops from the underground parts of the shoots and rhizomes, which are mostly present at an average depth of 0.5 m from the soil surface and can grow 1 m p.a. to a maximum of 10 m [Milke et al. (2020)]. This plant, considered native to North America, has largely accelerated its spread throughout the country over the past 150 years Saltonstall (2003). However, it has also expanded globally and is now one of the most common emerging species. This is largely due to the wide variety of characteristics it can possess and indeed its ability to adapt to many types of habitats, even under adverse environmental conditions [Milke et al. (2020)]. In addition, it can tolerate a wide range of temperatures and soils with anoxic conditions (typical of wetlands). Moreover, it is relatively resistant to underground saline conditions and to a wide pH

¹https://wiki.bugwood.org/Phragmites_australis#Bibliography

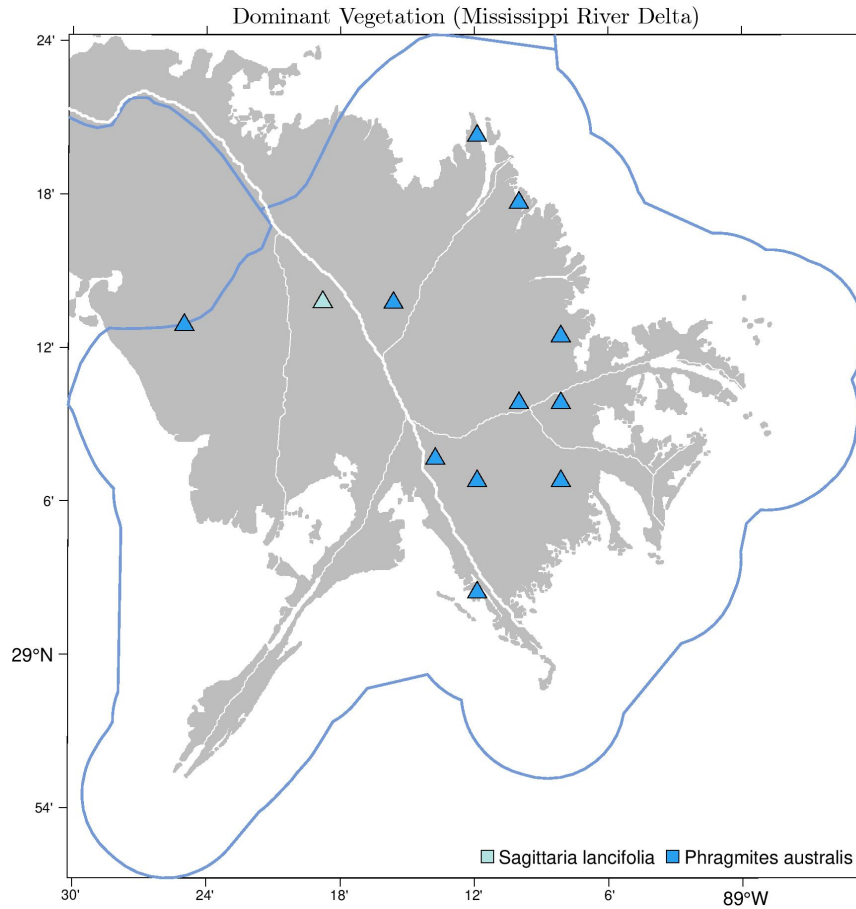


Figure A.1: Map representing the predominant vegetation for the different CRMS sites in the modern MRD. Only stations with available data are present.

range $(3.9-8.6)^2$.

To gain a more precise understanding of how *Phragmites australis* responds to salinity, a curve was fitted that describes how the relative growth rate (RGR), which indicates the rate of increase in dry weight per unit of dry weight of the plant [Youssef et al. (2023)], varies as the salt concentration C increases (Figure A.2).

The ‘*Sagittaria lancifolia*’ is another widely distributed species in the Birdfoot and is also known as the ‘Duck potato’ due to its large potato-shaped corms that form underground. It is defined as a herbaceous, aquatic, native, monocotyledonous perennial plant that commonly grows in swampy soils or standing water in ponds, lakes, streams and ditches and typically flowers in spring [Moore et al. (2016)]. The leaf system consists of lance-shaped leaves, which develop from underground rhizomes and can reach a length of 60 cm and a width of 10 cm. It produces distinctive, showy flowers consisting of three white petals and three green sepals. [Moore et al. (2016)].

²https://nas.er.usgs.gov/queries/greatlakes/FactSheet.aspx?Species_ID=2937

It is native to the wetlands of North America [Marburger (1993)], in particular in the southeastern United States, with a high concentration in all counties of Florida³. They grow in different soil textures, with greater biomass development (both over-soil and subsoil) in loamy sandy sites than in loamy clay sites of the upper Mississippi River [Clark and Clay (1985)]. It has been found to survive in regions where the depth of the water table is less than 50-60 cm and is adapted to different environmental conditions, surviving in fresh water with a PH ranging from 5.9 to 8.8 and an alkalinity between 0.5 and 297.5 mg/l as $CaCO_3$. It also manages highly calcareous waters, but is not considered salt tolerant [Marburger (1993)]. Also for this species, it was possible to graphically show the effect of salinity on it, and in this particular case, how its stem elongation (cm/week) varies with increasing salt concentration C (Figure A.2).

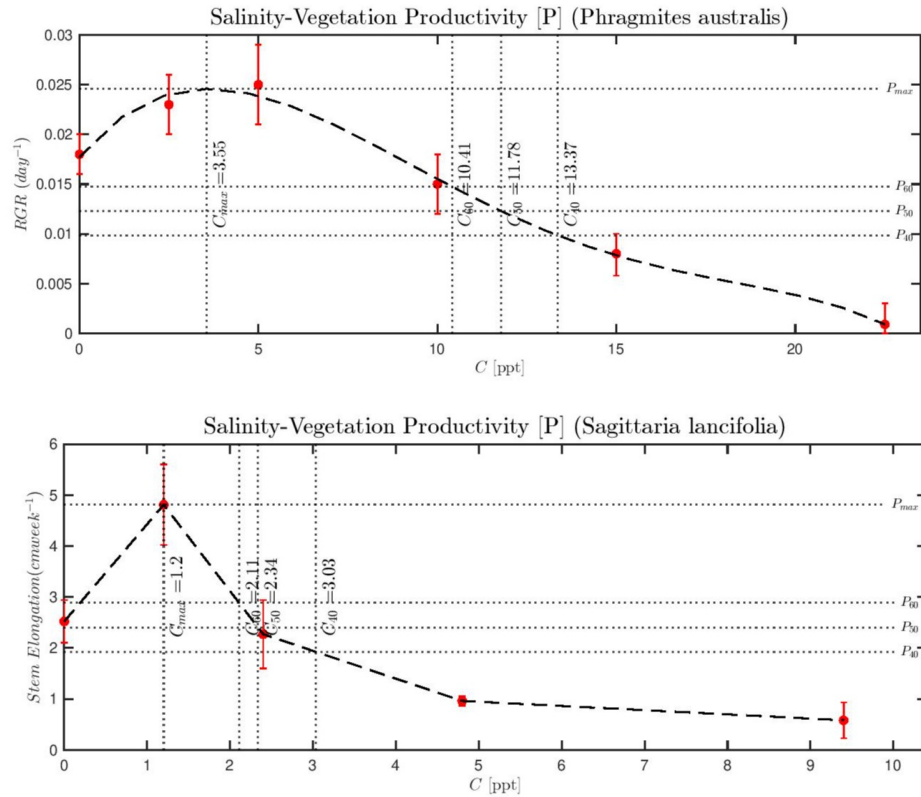


Figure A.2: The upper panel shows the evolution of RGR as a function of C-salt concentration, for the species *Phragmites Australis*. On the other hand, the lower panel shows how the salt influences the Steam Elongation (cm/week) of *Sagittaria lancifolia*. The data used were taken from the literature [Vasquez et al. (2006) and McKee and Mendelssohn (1989)] and represented as red dots with the corresponding error.

³<https://plants.usda.gov/plant-profile?symbol=SALA2>

Appendix B

Tools and methodologies for data collection

The instruments used for data collection are part of the Coastwide Reference Monitoring System-Wetlands¹ (CRMS), a system developed to monitor the health of Louisiana's wetlands. CRMS allows for the evaluation of individual restoration projects as well as the collective effects of multiple projects on the broader ecosystem. The system includes 392 monitoring sites established between 2006 and 2008 and each one is typically equipped with a hydrology station that tracks water elevation and salinity on an hourly basis. There is also a boardwalk that leads to stations measuring surface elevation change, vertical accretion, and soil porewater salinity, as well as a vegetation transect for collecting data on plant communities. In swamp sites, additional stations monitor forest canopy, understory, and herbaceous layers, while in floating marsh sites, stations for elevation change and accretion are replaced by those that monitor marsh mat elevation. The tools and methods for collecting the data used for the model are briefly described below, with all information sourced from Folse et al. (2018). With regard to open water table monitoring, the following are considered habitats where water can completely submerge the recording devices. In this case two different configurations are used:

- A treated wooden pole (10.16 cm x 10.16 cm x 609.6 cm) is driven deep into the substrate of water bodies such as bays and canals where the water depth is less than 243 cm. In addition, a perforated PVC pipe and electrical box are

¹<https://lacoast.gov/crms/>

mounted on a wooden board (5.08 cm x 10.16 cm x 304.8 cm) and attached to the wooden pole (Figure B.1).

- A single-pole system suitable for high-energy environments such as rivers, this system uses a stainless steel pipe with a plate welded to the bottom for stabilization. The pipe has multiple slots for effective water exchange.

Different types of sondes, such as the YSI 600XLM, are employed to measure the open water level while also recording important parameters like water temperature, specific conductance, and salinity. Since these probes are submerged, it is essential to determine the minimum water level during installation in order to ensure that they remain underwater during dry periods, preventing exposure that could result in inaccurate measurements [Folse et al. (2018)].

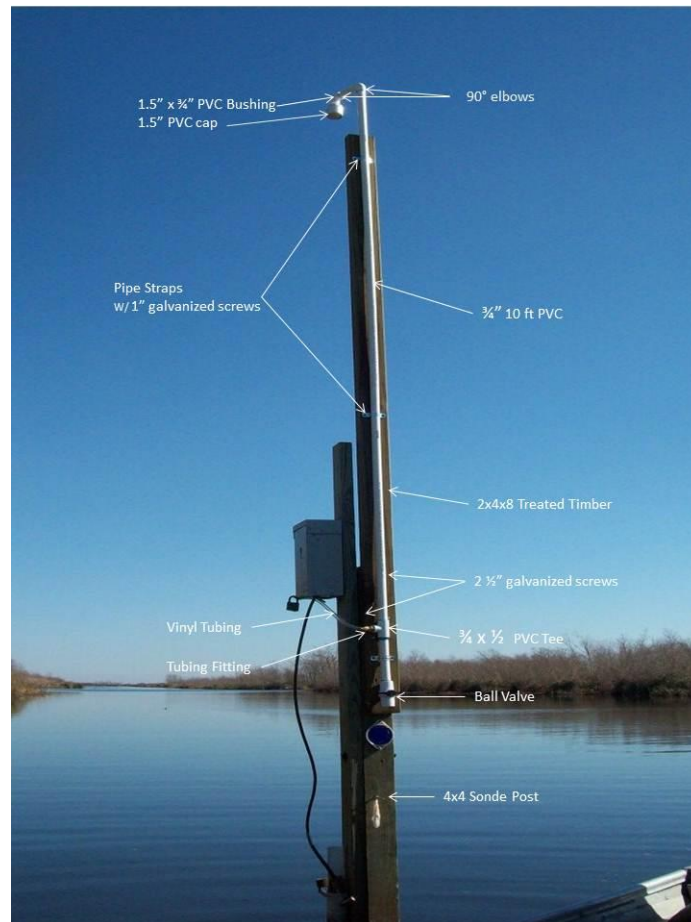


Figure B.1: Photograph of a CRMS station for measuring open water table level and other parameters. Reproduced from Folse et al. (2018)

The Marsh surface change is tracked using the Rod Surface Elevation Table (RSET)

and the marker horizon technique. The former is an accurate, non-invasive instrument used to monitor changes in surface elevation over time with respect to a fixed point in the subsurface (Figure B.3). The system involves inserting stainless steel rods into the soil (~ 20 m deep), penetrating the root zone, organic matter, and all softer underlying layers until resistance is met. These rods extend about 0.6 m above the surface, where they are stabilized by a surface-cemented pipe. A custom-made stainless steel collar is permanently attached to the rod, providing a relative (because the entire area is still subject to subsidence, which also affects the instrument itself) stable horizontal reference point for future consistent measurements and allowing the instrument to be reused for continuous monitoring at the same location. Data collection with the RSET involves attaching a custom-built table to the collar and then lowering nine fiberglass pins through the table until they touch the ground surface. The length of each pin above the table is recorded in millimeters, and it is this measurement that tells us the change in elevation. Also to have an areal measurement, the survey is taken from four different positions around the station at 90° intervals, resulting in 36 data points [Cahoon et al. (2002)].

Regarding the second technique, plot sets are established around the RSET boardwalk with feldspar spread on the surface to define the marker horizon (MH). The first three plot set (PS1) are sampled every six months for the first two year. After every two years, new plot sets (PS2 and so on) are established and sampling of the old plot sets is at every 1.5 years with an interim 1 year sampling. The sampling is done by cryogenic coring technique, where a probe is inserted in the marsh beyond the MH and the soil sample frozen with liquid hydrogen. The height of soil layer above the MH is measure and recorded [Folse et al. (2018)] (Figure B.2).

By combining RSET measurements with data from the Marker horizon technique, which only tracks surface accretion, it is possible to gain a complete understanding of the factors that influence elevation with greater reliability and accuracy. This integration of methods provides critical insight into both surface deposition and the subsurface dynamics that influence long-term elevation changes. Obviously, it is essential that the first RSET measurement take place on the same day as the creation of the accretion stations and that subsequent measurements are made at the same time as the accretion data are collected [Folse et al. (2018)].

Finally, vegetation assessment at Coastal Reference Monitoring System (CRMS) sites is used to evaluate the condition of wetlands, including both marshy and herba-



Figure B.2: Frozen soil column in which you can see the white feldspar horizon and the material accumulated above it. Reproduced from Folse et al. (2018)

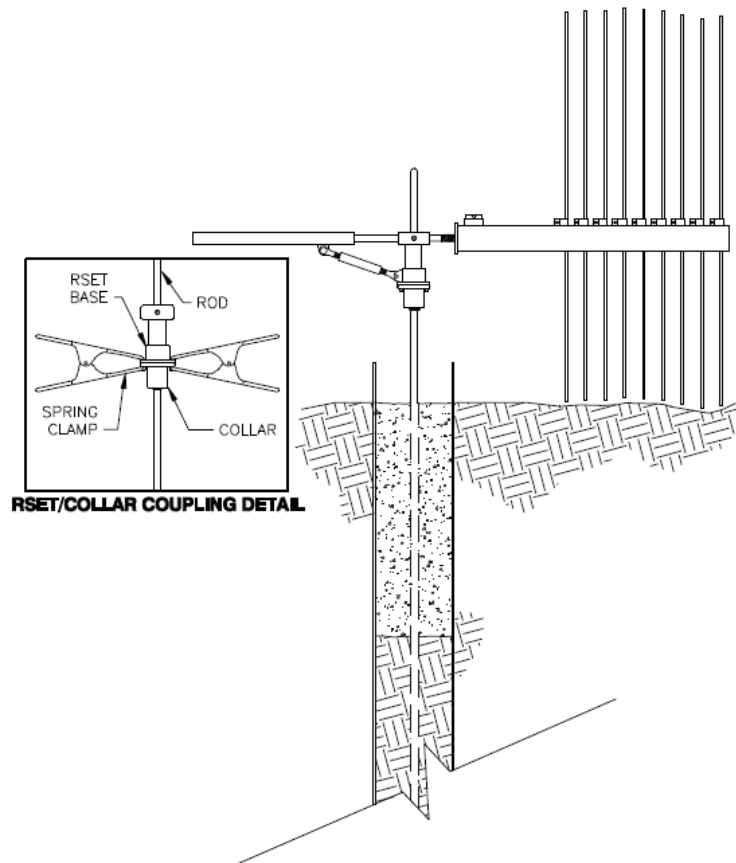


Figure B.3: RSET data collection scheme. Reproduced from Folse et al. (2018)

ceous types, through systematic sampling of the plant species present. In this process, sampling locations are chosen along diagonally established transects (that represent a good approximation for the entire site) within the monitoring zone (200 m²). Each location is marked with a PVC pole, and a 2x2 m square of PVC is utilized to outline the area under investigation (Figure B.4). Within the square, the percentage of overall vegetation cover is estimated, which encompasses herbaceous plants, shrubs, and vegetation mat layers. The coverage of areas devoid of vegetation (such as open water or bare soil) is also assessed. Species within the square are identified, and their percent cover is estimated. Plants that extend over the square, even if they are rooted outside, are included in the sampling. The height of the dominant plants and the depth of water or soil at the sampling sites are recorded. From these analyses, it is possible to discern the predominant vegetation present in a specific area for a given sampling interval [Folse et al. (2018)].



Figure B.4: Image of a herbaceous marsh vegetation station (2 m x 2 m) site along with a leveling rod for measuring the height of plants and the water level above the marsh structure. Reproduced from Folse et al. (2018)

Appendix C

Process for changing data due to subsidence

The Louisiana coast, particularly the MRD, has always experienced heavy sediment input from the Mississippi River. Over time, these sediments undergo compaction, creating two distinct sedimentary layers: Non-compressible Pleistocene sediments and Compressible Holocene sediments. This differentiation between layers significantly impacts the accuracy of instruments used to measure water levels (e.g., water level gauges) and surface elevation (e.g., RSET) [Heinrich et al. (2015)].

The RSET is typically installed at a depth of around 20 meters, while the water level gauge is installed at a shallower depth, between 4 and 5 meters Li et al. (2024). Since the water level gauge is primarily located in the compressible layer, it is more susceptible to shallow subsidence, which is generally more pronounced than deep subsidence. The depth at which the boundary between the compressible and non-compressible layers lies varies and tends to increase as one moves closer to the ocean due to increased sediment deposition Heinrich et al. (2015). This variation in depth leads to three possible scenarios [Li et al. (2024)] (Figure C.1):

- When both instruments are installed in the non-compressible layer, no corrections are necessary, as they are not subject to shallow subsidence, only to deeper, less significant subsidence.
- When the water level gauge is placed in the compressible layer and the RSET in the non-compressible layer, only the water level gauge experiences shallow

subsidence. In this case, a correction must be applied to the water level data to account for the differential subsidence between the two instruments.

- When both instruments are located in the compressible layer, a correction is necessary for both datasets, as the water level gauge, being installed at a shallower depth, will undergo more significant subsidence than the RSET. This requires corrections for both sets of measurements. This is typically the case in the Bird’s Foot Delta.

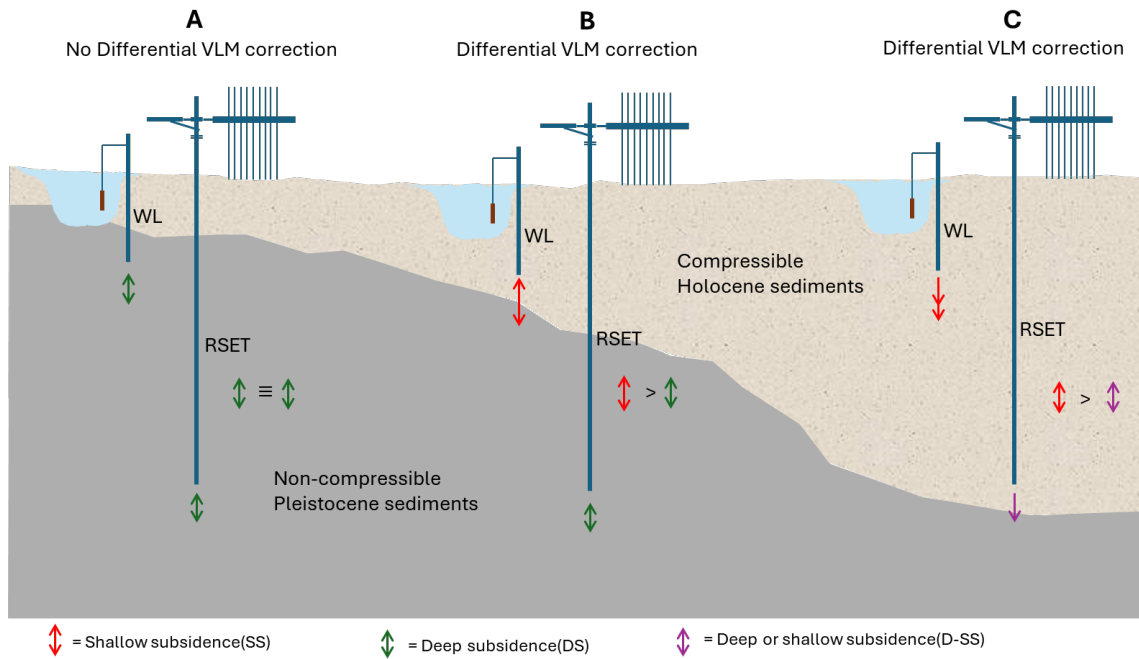


Figure C.1: The three possible scenarios regarding the subsidence of the RSET and the water level post. Adapted from Li et al. (2024)

According to Li et al. (2024) and reference in, the exact depth of the water level post installation is not certain, estimated to be between 4 and 5 meters, which complicates determining the precise corrective value to apply; however, it is understood that shallow subsidence is occurring. In Louisiana, the average shallow subsidence (SS) rate is 6.8 ± 7.9 mm/year, but studies indicate that the highest compaction rates occur between 1 and 3 meters, suggesting that subsidence at the water level gauge is likely lower than the average, as subsidence decreases with depth even within the compressible layer. The correction for vertical land movement (VLM) is assumed to follow a normal distribution, with the 95th and 5th percentiles being 4 mm and 1 mm, respectively, meaning there is a 95% chance that shallow subsidence is around

1 mm and a 5% chance it is around 4 mm. Corrective factors are randomly selected from this distribution, and since shallow subsidence causes a station to sink over time, corrections must be applied to data recorded prior to the most recent survey, conducted in 2021 for example presented below, while adjustments should also be made to current measurements, assuming a constant rate of depth variation (Figure C.2).

Even though the data adjustment process is complex, its role in ensuring the accurate interpretation of hydrological parameters and the true in situ conditions is essential.

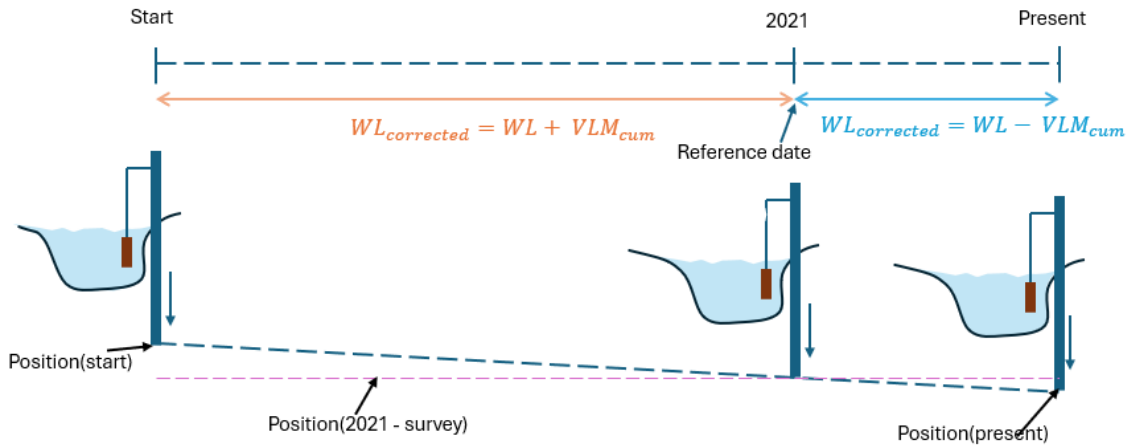


Figure C.2: Diagram indicating the correction of water level data to be implemented before and after the reference survey

Appendix D

Overview of Hydrological Conditions for MRD Stations

The following panels present in-situ data for the remaining Birdfoot stations that were not individually analyzed in Chapter 5.

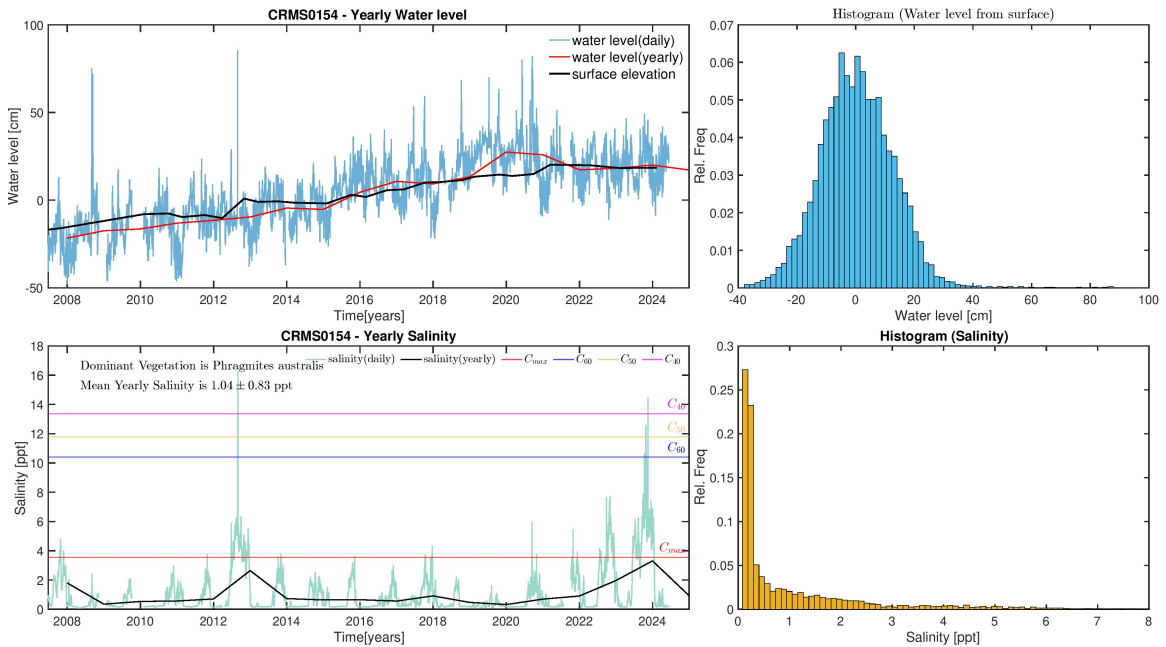


Figure D.1: Temporal variations in the water table and salinity at CRMS 0154, along with their corresponding probability histograms.

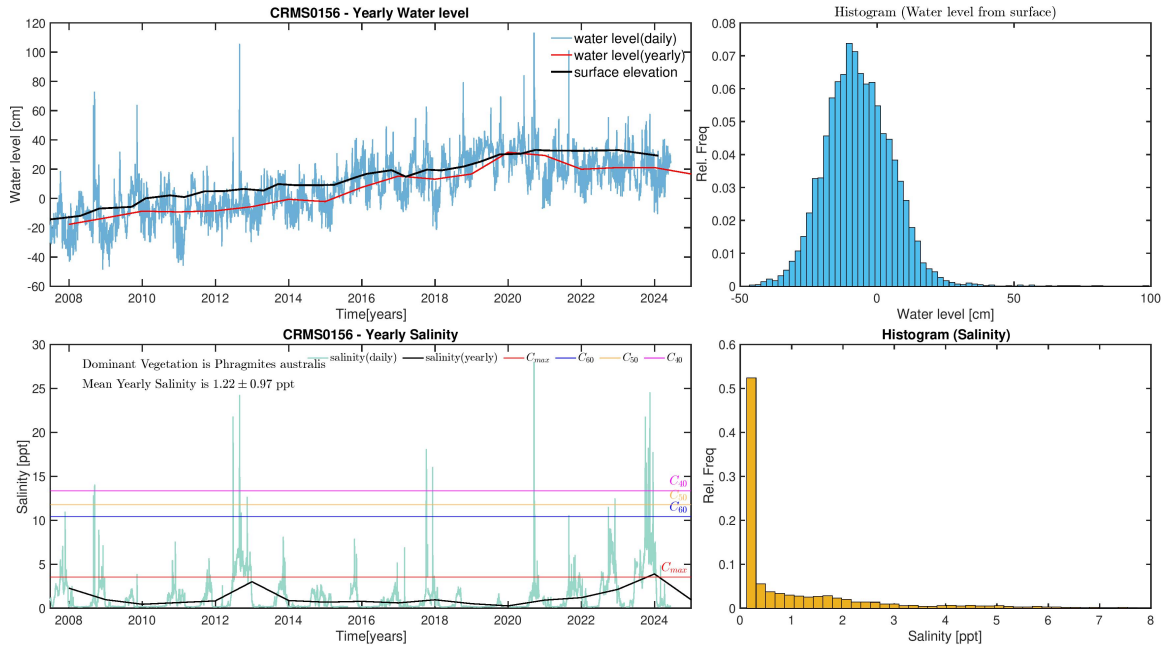


Figure D.2: Temporal variations in the water table and salinity at CRMS 0156, along with their corresponding probability histograms.

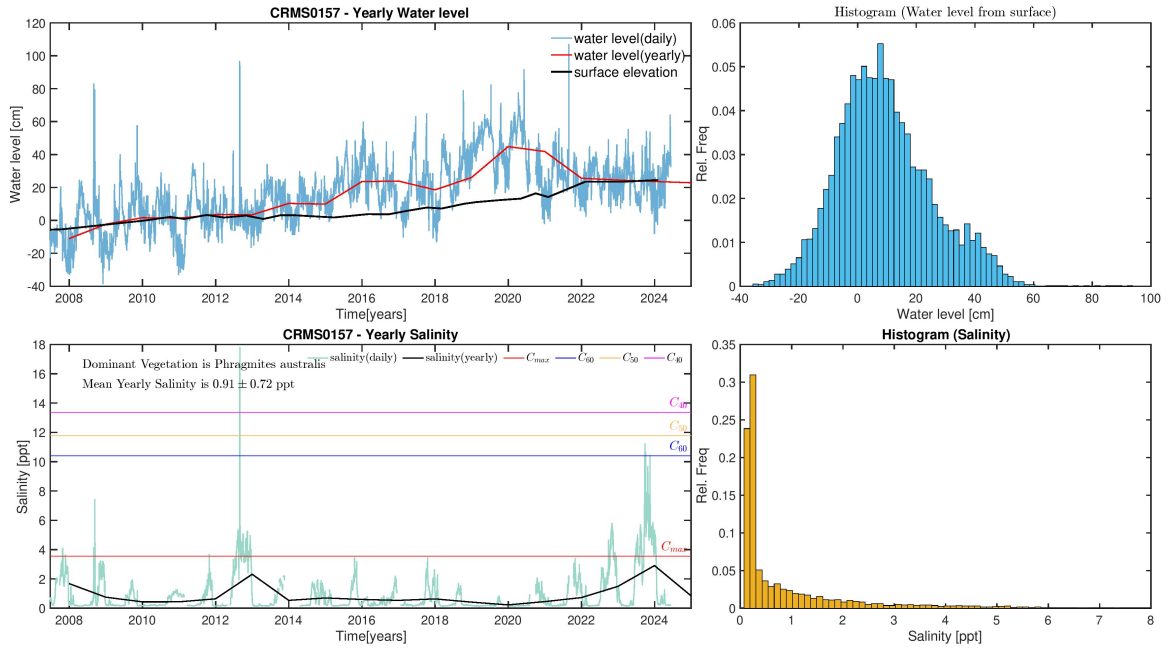


Figure D.3: Temporal variations in the water table and salinity at CRMS 0157, along with their corresponding probability histograms.

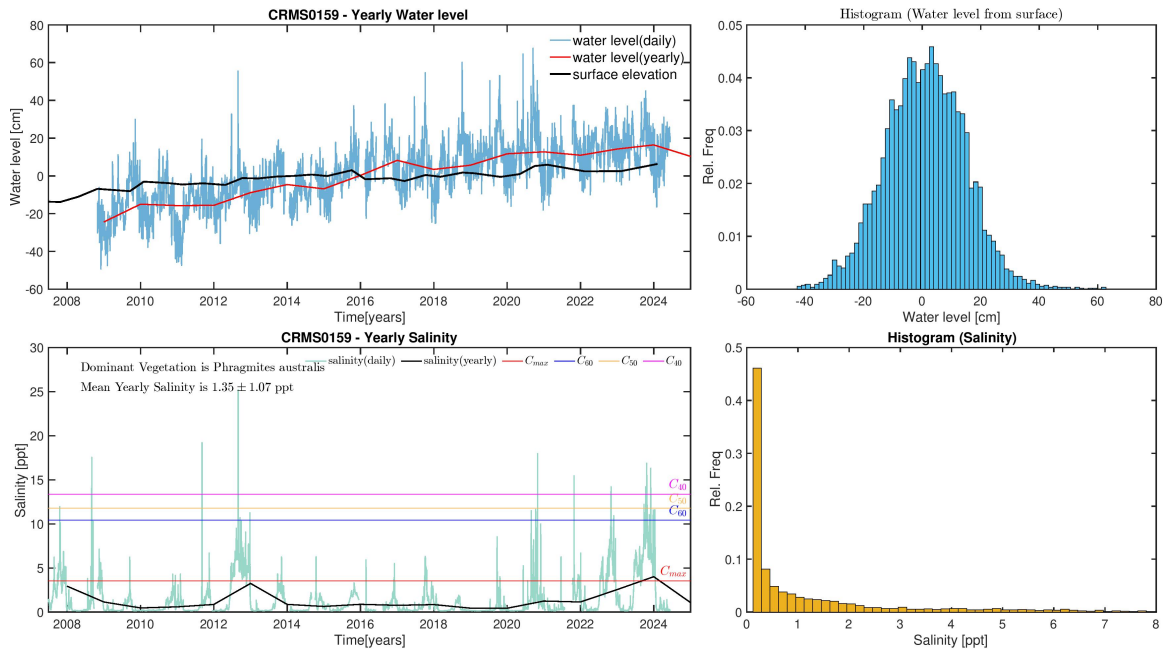


Figure D.4: Temporal variations in the water table and salinity at CRMS 0159, along with their corresponding probability histograms.

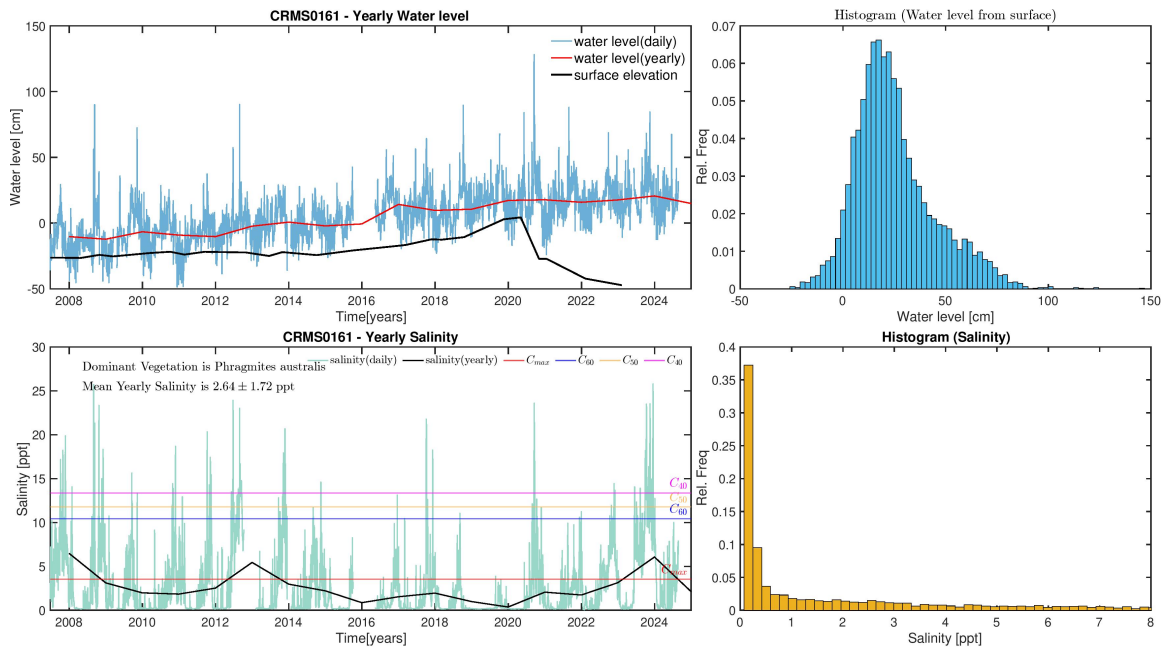


Figure D.5: Temporal variations in the water table and salinity at CRMS 0161, along with their corresponding probability histograms.

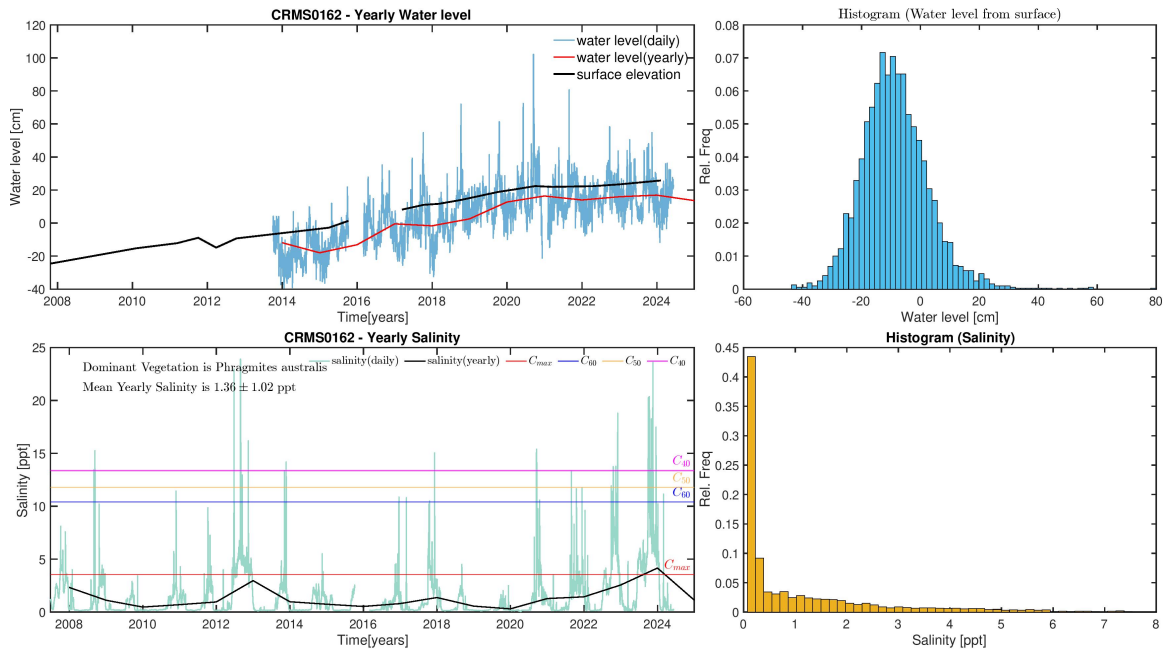


Figure D.6: Temporal variations in the water table and salinity at CRMS 0162, along with their corresponding probability histograms.

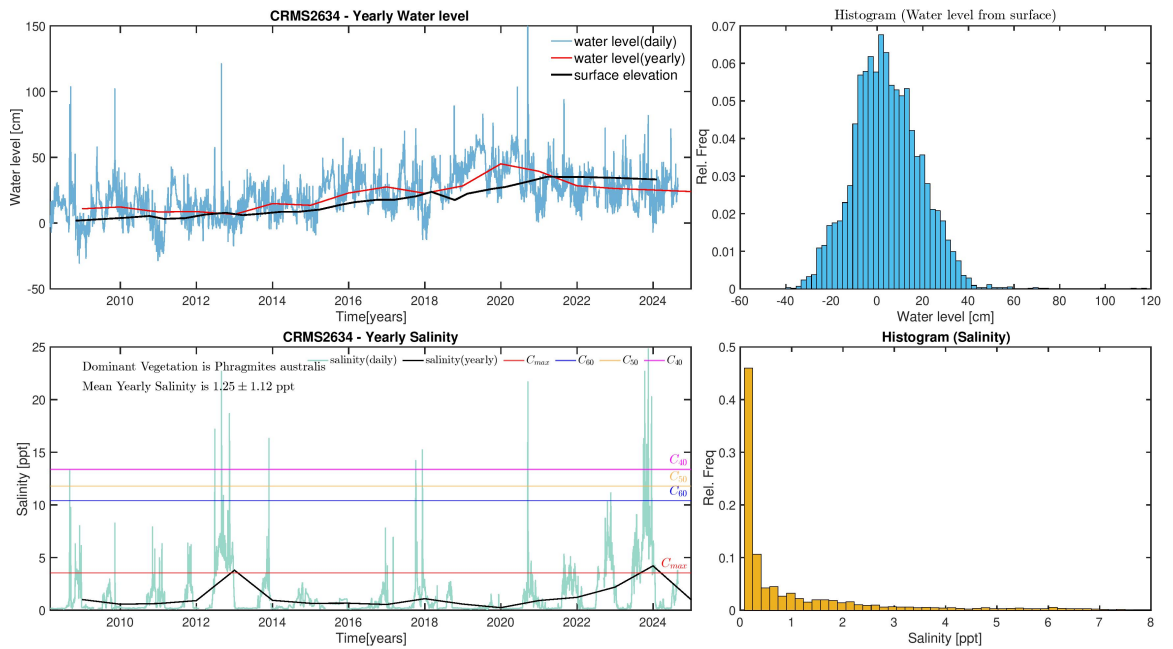


Figure D.7: Temporal variations in the water table and salinity at CRMS 2634, along with their corresponding probability histograms.